UiT The Arctic University of Norway

Faculty of Health sciences

Department of Pharmacy

Cell Signaling and Targeted therapy research group

Functional analysis of signaling pathways activated by Anisomycin and Dexamethasone in two different breast cancer cell lines

Rosaline Brown

Master's thesis in Pharmacy, FAR-3911, Fall 2021 – Spring 2022

Supervisors: Lisa Zeyen Øyås and Ingvild Mikkola, Department of Pharmacy, UiT

Acknowledgments

Abstract

Background: While targeted therapy exists for ER-positive breast cancers, the treatment option for TNBC is conventional chemotherapy giving a poorer prognosis. It is therefore of interest to study molecular mechanisms and differences between MCF7 (ER-positive) and MDA-MB-231 (ER, PR, and HER2- negative). These cell lines are *in vitro* representative models for luminal A (non-aggressive) and basal-like (aggressive) breast tumors. In this study, the cell lines are stimulated with Anisomycin and Dexamethasone, and their response is observed and compared in relation to the P38 MAPK signaling pathway and GR.

Methods: To achieve molecular and functional analysis of the cell lines Western Blot, proliferation assays, cell viability assays and a scratch wound assay was achieved to compare the cell lines, respectively.

Results: Anisomycin is a rapid and potent activator of p38 MAPK and inhibits proliferation in both cell lines, but the activation of the p38 MAPK signalling pathway is different as shown by the phosphorylation kinetics of the downstream targets GR (S134) and HSP27. Results also show that Dex stimulation and activation of GR in the MDA-MB-231 cells cause increased proliferation, but for MCF7 the effect of Dex with regard to proliferation was minor. Further, migration seemed to be positively affected by Dex in MCF7 and negatively affected by Dex in MDA-MB-231 cells.

Conclusion: These findings indicate that activation of the p38 MAPK pathway in MCF7 and MDA-MB-231 cells will cause different downstream responses, among them the kinetics of the phosphorylation of GR. It will be interesting to see if these differences could be further investigated with the intention to develop targeted therapy for TNBC cells.

Abbreviations

Ani	Anisomycin
Dex	Dexamethasone
ER	Estrogen receptor
GR	Glucocorticoid receptor
HER2	Human epidermal growth factor receptor 2
hrs	hours
HSP27	Heat Shock Protein 27
IF	Immunofluorescence
kDa	kilo Daltons
l	Liter
MAPK	Mitogen-Activated Protein Kinase
MAPKK	Mitogen-Activated Protein Kinase Kinase
MAPKKK	Mitogen-Activated Protein Kinase Kinase Kinase
MK2	MAPK - activated Protein Kinase 2
mg	milligram
ml	milliliter
min	minutes
MW	Molecular weight
nM	Nanomolar
PR	Progesterone receptor
rpm	rounds per minute
sec	seconds
TNBC	Triple negative breast cancer

μg	microgram
μl	microliter
WB	Western blot

Table of Contents

1 Introduction

The estrogen-dependent cell line MCF7 and the triple-negative mutant cell line MDA-MB-231 are appropriate cell culture models because they represent clinical variations of breast cancer that are detectable in patients. Previous observations have already proved that these cell lines respond differently to certain stress signals and chemotherapeutic drugs on a molecular level. This thesis focuses on a comparison between these two cell lines, that also include the functional differences between them. The comparison will be investigated by focusing on the p38 MAPK signaling pathway and GR in response to the stimulations of anisomycin and dexamethasone.

1.1 Breast cancer

Breast cancer is a disease characterized by an uncontrollable growth of cells in the breast. It is a heterogeneous collection of different diseases clinically and molecularly. It is diverse in cell morphologies, molecular phenotypes, drug responses and with notable differences in patient survival (1). Breast cancer affects both genders, but the female gender has a higher risk of developing the disease. It is rare for men to develop breast cancer and approximately 0,5 – 1% of breast cancers occur in men (2).

Breast cancer is one of the most diagnosed cancers among women in the world. In 2020, 2,3 million women were diagnosed and 685 000 died due to the disease. At the end of 2020, the number of women diagnosed with breast cancer in the past 5 years was 7,8 million (2). Breast cancer is therefore one of the most prevalent and diagnosed cancers, and it is considered one of the leading causes of cancer-related deaths among women worldwide (3).

1.1.1 Anatomy and pathology

The breast is an exocrine mammary gland that is responsible for the production and secretion of milk to nourish an infant. The breast is composed of the thoracic wall, pectoralis minor,

Adipose tissue, breast lobule, lactiferous ducts, areola, and nipple. Structurally, the mammary glands are present in both sexes, but only functional in the females (4, 5).

The biological function is made possible by the lobes that contain lobules, where the lobules are connected to a lactiferous duct. The lactiferous ducts are responsible for transporting milk from the lobules to the nipple from where it can be released.

Estrogen and progesterone are the key hormones that affect the breast, but other hormones like glucocorticoids, insulin, and prolactin also have an impact on breast tissue regulation as well (4). From the early stages of birth to the ending stage of menopause, there are a lot of hormonal changes in the female breast. These hormonal changes can be an explanation for why breast cancer is more common among women than men, because women have more physiological changes in the breast that are heavily influenced by hormonal changes (6).

Breast cancer occurs when the mammary gland forms a malignant tumor (6). The tumor can be found in the ducts (ductal breast cancer) or the lobules (lobular breast cancer). The characterization of the tumor is based on how likely it is to spread to the other parts of the breast or body. Non-invasive breast cancer normally does not spread to other parts of the body, an example is ductal carcinoma in situ (DCIS), which stays in the ducts of the breast. Invasive breast cancer is much more common and spreads to lymph nodes or other parts of the body, an example is invasive lobular carcinoma (ILC) (7).

1.1.2 Classification

There are four tumor subtypes of breast cancer: Luminal A, Luminal B, human epidermal growth factor receptor 2 overexpressing (HER2 positive), and triple-negative breast cancer (TNBC). TNBC can be differentiated into basal, Claudin low, metaplastic breast cancer and interferon–rich (8), (Figure 1)

Luminal breast cancer cell lines are characterized by a positive expression of the estrogen receptor (ER) and/ or the progesterone receptor (PR). Most studies do not differentiate luminal cells into a luminal A and B cell line, but observations of cells in luminal B tumors are in principle more invasive and therefore more aggressive than luminal A cells. HER2-positive cells bridge the gap between luminal and basal cell lines, are heterogeneous and encompass

both luminal and basal features. HER2 overexpression is shown to be associated with ER downregulation (8).
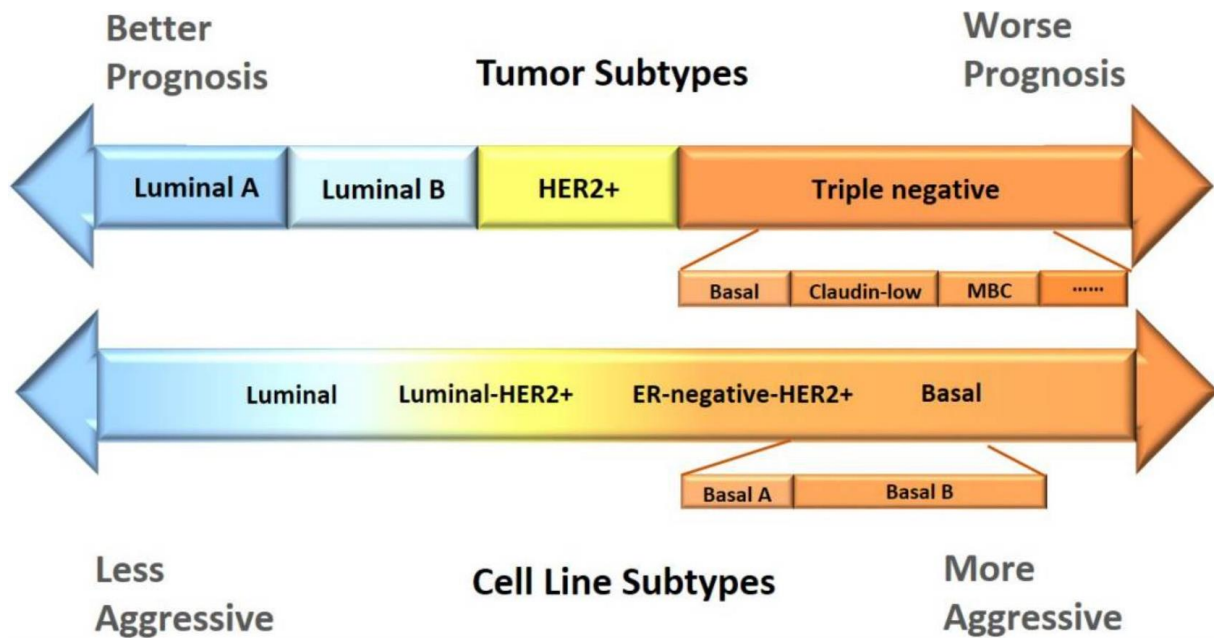
Figure 1: *Comparison of the current subtyping schemes between breast cancer cell lines and tumors. (Figure is taken from reference 8)*

TNBC is the most heterogeneous among all subtypes. It is characterized by the absence of ER, PR and HER2, and the cell lines are classified as basal A and basal B in most literature. Basal A is more luminal-like, and basal B is more basal-like. TNBC tumors can be further differentiated into basal, claudin-low, MBC (metaplastic breast cancer) and interferon-rich. (8). TNBC counts for 10 – 20 % of newly diagnosed invasive breast cancers (9).

Luminal tumors have a better prognosis because the luminal cell lines are less aggressive than that in triple-negative tumors and cell lines (8). *In vivo* and *in vitro* studies that use various breast cancer cell lines have established a large proportion of current knowledge on breast cancer (8).

1.1.3 Treatments

Breast cancer treatments prevent cancer growth and metastasis, and the results mainly save the life of patients. When the disease is identified early, treatment can be highly effective (2). The treatments consist of surgery, radiation therapy and medication (hormonal-, chemo-, targeted biological- and immunotherapy) (2). There are several effective targeted therapies available for luminal and HER2-positive tumors. Most breast cancer treatment focuses on the assessment of receptors, most notably ER, PR and HER2 (4).

However, triple-negative breast cancer is a challenge to treat, due to its particularly aggressive character. Specific molecular targets are missing on TNBC, so general treatment consists of systemic chemotherapy (10) but observations conclude that current chemotherapy treatments for TNBC lead to poor prognosis and drug resistance (11). Conventional chemotherapy treatments are costly and have many side- effects (6). Numerous studies are investigating a wide range of potential targets in TNBC and creating a novel class of anti-cancer therapy e.g. Poly (ADP-ribose) polymerase inhibitors (PARPi) (12). PARPis are targeted therapies that are approved by the FDA and EMA for patients with BRCA1 and BRCA2 mutations (13). PARP proteins are involved in the repair of single-stranded DNA, and PARPi inhibits PARP proteins. Inhibited PARP proteins in BRCA1 and BRCA 2 mutated cells leads to apoptosis. Recent results also show that some TNBC cell lines were susceptible to PARPi regardless of the BRCA-status (14). There is still room for more therapeutic approaches that can lead to effective treatment of TNBC to improve the outcome for patients.

1.1.4 MCF7

The MCF7 cell line is a human breast cell line that was derived from the pleural effusion of a 69 year old Caucasian woman with metastatic breast cancer (adenocarcinoma) in 1973 at Michigan Cancer Foundation, Detroit (6, 15). This cell line is ER and PR positive and belongs to the luminal A molecular subtype. It has wild-type p53. It is a poorly aggressive and non-invasive cell line and is normally considered to have low metastatic potential. This cell line has produced more data of practical knowledge for the development of therapies than any other breast cancer cell line (8, 15).

1.1.5 MDA-MB-231

MDA-MB-231 is the most commonly used TNBC cell line for studying cancer metastasis (1). This cell line is represented as a good model of TNBC because it is ER-, PR-, HER2-, cadherin negative and expresses mutated P53. In vitro, the cells show an invasive character (10) and can be classified as basal B, claudin-low or even mesenchymal-like tumors (8). MDA-MB-231 is isolated from pleural effusion of a patient with invasive ductal carcinoma at the M D Anderson Cancer Center and is frequently used to model late-stage breast cancer (10).

1.2 Cell cycle

All living organisms' fundament is based on self-reproduction. All cells reproduce by dividing in two, where each parental cell divides into two daughter cells. The daughter cells grow into parental cells, divide and give rise to a new cell population. This process aptitude cells to proliferate, so the division of all cells must be carefully regulated and coordinated with both cell growth and DNA replication order. (16).

1.2.1 Phases of the cell cycle

The cell cycle process can be divided into two basic parts: mitosis (nuclear division) and interphase. Interphase is the time during which both cell growth and DNA replication occur, so cell division can be completed. The cells grow at a steady rate throughout the interphase, however, the DNA is synthesized during only a portion of the interphase. In eukaryotic cells the timing of DNA synthesis divides the cell cycle into four coordinated processes that include cell growth, DNA replication, distribution of duplicated chromosomes to daughter cells and cell division. The four coordinated processes in the cell cycle has generated four separated phases called G1, S, G2, and M (16) (Figure 2).

The G1 phase: The interval between mitosis and initiation of DNA replication. The cell is metabolically active and continuously grows.

S phase: (Synthesis), this is where DNA synthesis is initiated and completed, resulting in DNA replication and duplication of the genome.

G2 phase: Cell growth continues in G2, and proteins are synthesized in preparation for mitosis. The replicated DNA is checked for mistakes.

M phase: In this phase the cell partitions the two copies of the genetic material into daughter cells. The division is completed due to cytokinesis, which results in two cells, and a restart of the cell cycle in each of the daughter cells.

Furthermore, the cell cycle also has a resting state called G0 (G zero), it is used as a non-proliferative state, and a cell can remain in G0 permanently or temporarily. Lack of nutrients is e.g that can make cells enter G0 (17).
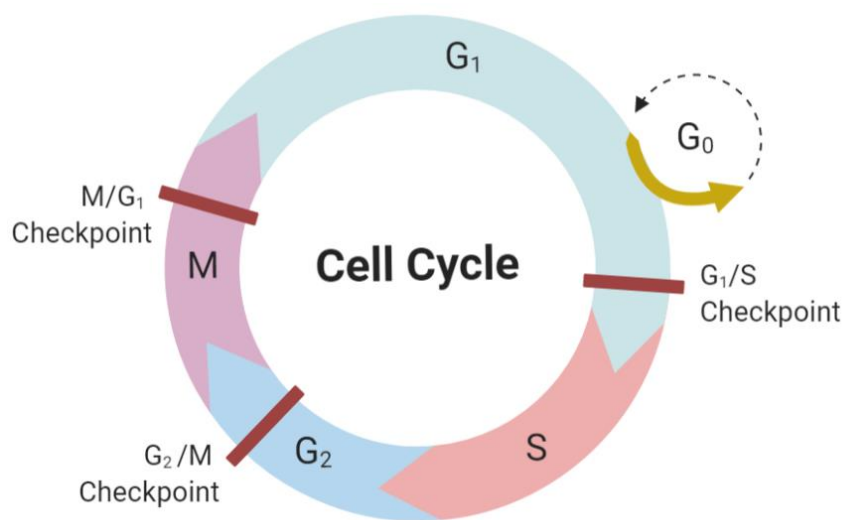
Figure 2: Illustration of the cell cycle with cell cycle checkpoints. (Cell cycle template taken from biorender.com)

1.2.2   Cell cycle regulation

The cell cycle is composed of cell cycle checkpoints (Figure 2). The cell cycle checkpoints prevent catastrophic cell division that results in daughter cells failing to inherit complete copies of the genetic material. Several checkpoints function to ensure that complete genomes are transmitted to daughter cells (16). DNA damage checkpoints in G1/S and G2/M lead to cell cycle arrest in response to damaged or unreplicated DNA. The spindle assembly checkpoint leads to a cell cycle arrest in the M-phase if the chromosomes are not properly aligned on the mitotic spindle (16, 18). In a mammalian cell cycle, these checkpoints are regulated by cyclin-dependent kinases CDKs, cyclins, and ubiquitin ligases. These regulators prevent entry into the

next phase of the cell cycle, through cell cycle arrest until the events of the preceding phase have been completed.

These regulators guard the genomic integrity by multiple checkpoints and inhibitors. They can pause or stop cell cycle progression in presence of DNA damage, when chromosomes are not sufficiently aligned in mitosis, or in the presence of inappropriate environmental stimuli (18). The cell cycle checkpoints can arrest a cell temporarily to allow

(I)   Restoration when cellular damage has occurred.

(II)   The dissipation of an exogenous cellular stress signal.

(III)   Availability of essential growth factors, hormones, or nutrients (19).

If cellular damage cannot be repaired, the regulators of these checkpoints may also result in the activation of pathways leading to apoptosis (16, 18, 19). Defects in cell cycle checkpoints can result in gene mutations, chromosome damage, and aneuploidy, all of which can contribute to tumorigenesis (19).

In the G1 phase, the cell cycle regulation starts with the formation of cyclin D (cyclin D1, cyclin D2 and cyclin D3) and CDK4/6 complexes (17). These complexes phosphorylate and partially inactivate Rb protein (Retinoblastoma), altering its conformation and resulting in the activations of genes that are required for entering the S phase (17, 18). Upon DNA damage there is an upregulation of the protein p53, a transcriptional regulator that activates the gene encoding a CDK inhibitor (CDKi), called p21. The protein p21 binds to the cyclin-CDKs complexes and prevents them from entering the S phase. This arrest gives the cell time to repair the DNA repair, and the repair is not possible the cell results in apoptosis(17). Defects in cell cycle regulation are a common cause of the abnormal proliferation of cancer cells, so studies of the cell cycle and cancer should be interconnected (16).

1.2.3   P53

TP53 is known as a tumor-suppressing gene and encodes the protein P53 that is involved in regulating the cell cycle (20). Upon activation, P53 can bind to specific DNA response elements and regulate the expression of genes responsible for cell cycle arrest, DNA repair, apoptosis, senescence, autophagy, ferroptosis and metabolism (20, 21).

P53 is normally expressed at low levels due to its short half-life and regulation of a series of regulators. MDM2 is an E3 ubiquitin ligase responsible for the degradation of P53 in wild-type cells, and the most identified negative regulator of P53 (19-23). MDM2 is normally bound to the protein in a P53-MDM2 complex (19-23). Whenever DNA damage occurs in a wild-type cell, DNA damage response (DDR) kinases phosphorylate P53, resulting in a disconnection from MDM2 and an upregulation of P53 (21, 23, 24). The phosphorylation and increased concentration of P53 activate its function, and the output can be summarized as homeostasis, repair or cell death (20). Subsequently, P53 initiates its degradation by activating MDM2 transcription, creating a P53-MDM2 negative feedback loop (20).

P53 can induce cell cycle arrest at several phases in the cell cycle, by regulating genes required for progression through G1/S and G2/M checkpoints (15). In the M phase of the cell cycle, P53 directly regulates the duplication of centrosomes so proper segregation of chromosomes can occur (20). P53's ability to induce cell cycle arrest or apoptosis in cells after DNA damage indicates that it might prevent cancer by preventing the accumulation of oncogenic mutations (21).

It appears that several factors influence how the cell interprets and responds to P53 activation, and it is puzzling why P53 promotes cell cycle arrest in some cell types and apoptosis in others (21). Considering previous research, it is surprising that there is no clear and simple answer to the question of what P53 exactly does and how. P53 is encapsulated in a massively populated and interconnected network of regulators and effectors that enables a flexible P53 response coordinated to fit cell types and conditions at the time of activation (21). Cellular context like cell type, epigenetic state, tissue microenvironment and activating signal is central to both the biochemical aspects of P53 activity as well as the biological outcome of a P53 response (21).

In human cancer, the *TP53* gene is the most commonly mutated gene (20, 21, 23), and around 50% of human tumors have a P53 mutation and the exact mutation rate varies according to the tumor type (22). Previous observations inform that mutant P53 has an increased half-life compared to wild-type P53 and that the high basal level of P53 expression observed in many tumor cells was indicative of mutant P53 (19). Mutations in *TP53* not only impair its antitumor activity, but also permits mutant P53 protein with oncogenic properties (22, 23). An impaired function of P53 dysregulates cell cycle regulation (21). The mutations of P53 results into an advantage for the tumor cells, allowing them to evade cell cycle checkpoints, avoid apoptosis and senescence, and proliferate under conditions where normal cells cannot.

In spontaneous breast cancers, *TP53* mutations are mostly found in the TNBC subtype when a *TP53* mutation is not truncal or initial (20). Observations also indicate that both inherited and spontaneous BRCA1 and BRCA 2 mutations are commonly followed by TP53 mutations. 70 – 90% of cancers with BRCA1 mutations have TP53 gene mutations. Although BRCA 2 mutation shows signs of DNA damage, TP53 mutations are less frequent in cells including BRCA 2 mutation compared to BRCA1 mutated cells. (20)

Existing evidence postulate that P53 is a good molecular target for cancer therapy (23). Unfortunately, there are several important complexities of the P53 pathway that have not been elucidated in detail, including the mechanism of action, phenotypes of the mutant P53 protein and their role in cancers. The incomprehensibility of this gene and its protein precludes the aim of taking advantage of the P53 pathway to produce an effective therapy (20, 23). Therefore, more research is needed to have sufficient information that can enable the utilization of the P53 pathway and improve cancer therapy.

1.2.4 Cell signal transduction

Cells must interpret the multitude of signals they receive from their environment and other cells to help coordinate their growth, function and maintenance (17). In cell biology, signal transduction is defined as a process where a cell responds to an extracellular signal. The signal transduction pathway will transfer the signal from a cell's exterior to its interior.

Different cells can receive specific signals through structures on their surface called receptors. After an extracellular interaction with these receptors, the signal travels into the cell and results in an intracellular signal, which is generally organized through a biological signaling pathway. A biological signaling pathway consists of a series of actions among molecules in a cell that leads to a certain product or a change in the cell. Habitually the formation of protein-protein complexes are important for many biological processes, including signal transduction (25, 26).

Signal transduction is when a chemical signal from outside the cell might direct the cell to produce a particular molecule e. g. protein inside the cell. In turn, that protein may be a signal that prompts the cell to take an action. Signal transduction is in essence an exterior message being transmitted by specialized proteins through biological pathways that trigger a specific

cellular response. Cell signal transduction is composed of a balanced and regulated system (17, 26).

1.3 P38 MAPK

Mitogen-Activated Protein Kinases (MAPKs) have been identified as a family of kinases that are highly implicated in different cancer processes. (27). The MAPK family is important for the signaling transduction of extracellular and intracellular signals in different responses at the cellular level. Currently, three main groups of MAPKs have been identified in mammals: The extracellular signal-regulated kinases (ERK), Jun N-terminal kinases (JNK), and p38 MAPK (27).

MAPK signal transduction pathways are ubiquitous and highly conserved in eukaryotic, and they promote coordinated and integrated responses to numerous stimuli through receptor protein kinases (RTKs), leading to important cellular and physiological effects(27, 28). The MAPK signaling pathways are cascades of kinases, and are regulated by phosphorylation cascades which phosphorylate MAPK (27). Primarily, two serially activated protein kinases (MAPKKK and MAPKK) result in the activation of a MAPK (27, 29).
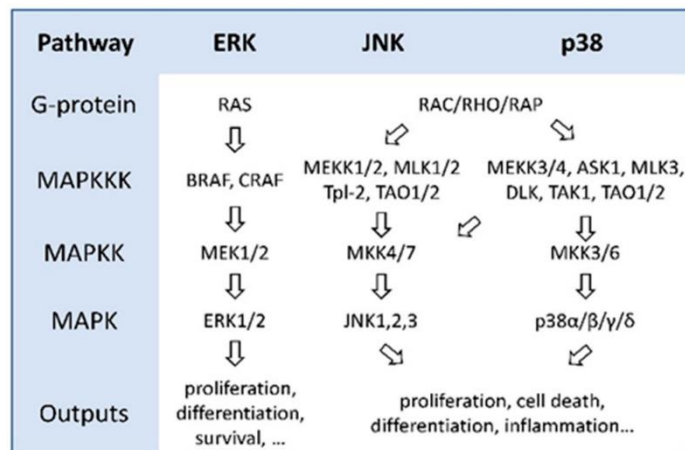

Figure 3: *Organization of MAPK pathways. The MAPK core consists of three kinases (MAPKKK, MAPKK, and MAPK), which form a signal transduction cascade that receives input from G-proteins, that are activated by receptor tyrosine kinase (RTK). RTKs are not in figure. (Figure is taken from reference 29)*

In mammals, MAPK p38 can be found both in the cytoplasm and in the nucleus, and its location determines its signal specificity (27). p38 exists in 4 isoforms: p38α, p38β, p38γ, and p38δ, encoded by four different genes, whose protein products have overlapping and isoform-specific functions (29, 30). The main MAPKKK generally activates the p38 pathway in response to stress (27). The isoforms are collectively activated in response to different stresses produced in the cellular environment as well as the liberation of inflammatory cytokines such as interleukin-1 (IL-1) and tumor necrosis factor-alpha (TNF-α) in processes of oxidative stress during UV radiation exposition, hypoxic conditions, or during ischemia (27).

MAPK p38 can e.g., control P53 activation, cause cell growth control, apoptosis, induce the immune system modulation, and generates a specific response to DNA damage. The phosphorylation of P53 by p38 regulates the G2/ M transition, and P38 can also repress cell cycle progression in G1 (27). Most studies have suggested that P38 regulates the inhibitors or activators of transcription, in addition to chromatin modulation, favoring or not the transcription of many genes implicated in different cellular processes (27). Ultimately, it is likely that the different effects of p38 pathway activation depend on cell type differences, along with the duration, quality, and intensity of the stimulus and its communication and interaction with other signaling pathways (27).

P38α can phosphorylate a variety of substrates in the nucleus and cytoplasm, and the activation of p38 α is often linked to MK2. MK2 is an example of a downstream subtract of p38. MK2 can target other transcription factors that are not directly targeted by p38 (27). Previous observation revealed that p38α activation can regulate MK2 protein levels, which, in turn, have a key role in the pathway output (25).

Normally p38α forms a complex with MK2 in non-stimulated mammalian cells, and upon pathway activation in response to mild stress or physiological stimuli, the pathway is transiently activated, allowing reformation of the p38α–MK2 complex and concomitant cell survival. However, cells treated with severe stress show sustained p38α activation, which phosphorylates MK2, subsequently dissociates the p38α–MK2 complex and degrades MK2. This results in an irreversible loss of MK2 and cell death (25).

Heat shock protein 27 (HSP27) is a downstream target of MK2 and plays a significant role in the inhibition of apoptosis and actin cytoskeletal remodeling (31). HSP27 is frequently overexpressed in many cancers and is associated with a poor prognosis, as well as treatment

resistance. Observations showed that phosphorylating HSP27 through MK2 inhibits its ability to promote early breast cancer dissemination (32). The activity relations of the p38-MK2-HSP27 pathway seem to be a promising target for diagnostic marker and potential therapy route in breast cancer (32).

p38 is considered a promising target, either using p38-specific inhibitors alone or in combination with other chemotherapeutic agents. However, the p38 isoforms can promote both pro-oncogenic and tumor-suppressive processes. As a consequence of p38's dual role in cancer, most studies support the idea that therapeutic inhibition of the p38 MAPK pathway must depend on the cellular context, cancer type, and tumor stage, as well as the intensity and duration of the signal, together with cross signaling between MAPK pathways (27).

Considering p38 is involved in many biological activities, its inhibition could lead to unwanted and unknown side effects, therefore efforts are currently focused on discovering agents that specifically target p38 or a component of the pathway that is deregulated and is the trigger for a particular disease. Previous observations ensure MK2's significant role in cancer development and/or cancer progression (24). Unlike p38, MK2 inhibition has been proposed as an alternative to reduce unwanted effects (27).

1.3.1.1 Anisomycin

Anisoymycin (Ani) is a pyrrolidine antibiotic isolated from cultures from various *Streptomyces griseolus* (33, 34), and commercially available under the name flagecidin for the treatment of plant pathogenic fungi (34). Previous studies identify Ani's potential to induce apoptosis of various cancers (35, 36). Combination studies also demonstrate that Ani provides a synergistic effect where it remarkably enhances the inhibitory effects of anti-cancer agents in many different cancer types (35).

The primary mechanism of action is due to the inhibition of protein synthesis via specific binding to the 60S ribosomal subunit, resulting in a suppression of polypeptide chain elongation (34, 35). Ani can induce ribo-toxic stress response and apoptosis in mammalian cells by activating the stress-activated protein kinase subfamily of MAPKs, including p38 MAPK (35-37). Therefore, Ani is also identified as an agonist of p38 MAPK in mammalian cells.

1.4 Glucocorticoid receptor

The glucocorticoid receptor (GR) is an intracellular receptor protein that belongs to a family of nuclear hormone receptors that are ligand-dependent transcription factors. These receptors are involved in activating and repressing gene expression, thereby affecting proteins and regulating key signaling pathways (9, 38).

The human GR (hGR) most common isoforms are hGRα and hGRβ, with MW 97 and 94 kDa. hGRα represents the classical bioactive glucocorticoid receptor that functions as a ligand-dependent transcription factor. hGRα is widely expressed in almost every human tissue and cell and resides in the cytoplasm. hGRβ is also widely expressed, but in lower concentrations, and primarily in the nucleus of cells It is not ligand-bound and therefore transcriptionally inactive. hGRβ functions primarily as a dominant-negative inhibitor of hGRα (38).

Upon hormone binding, the GR undergoes an allosteric change. Its new conformation exposes the receptor's nuclear localization signals and mediates translocation to the nucleus. In the nucleus, the activated receptor forms a homodimer and binds to glucocorticoid response elements (GREs) located in the promoter region of target genes (38, 39). This mechanism sends signals to the transcription machinery and regulates the expression of glucocorticoid-responsive genes positively or negatively, depending on the GREs sequence and promoter context. It's believed that GR dimerization affects downregulation, subsequently, after GR transcriptional activity it undergoes proteasomal degradation within the nucleus (44).

The receptor can also modulate gene expression as a monomer, independently of GRE binding, by physically interacting with and activating other transcription factors. GR has the potential to be phosphorylated at several sites. There have been reports of phosphorylation occurring on seven residues on GR: serine (S)113, S134, S141, S203, S211, S226, and S404 (40). GR can also be phosphorylated by MAPKs. MAPKs can modulate GR transcriptional activity (38). E.g. p38 MAPK phosphorylates GR S134, inhibiting GR nuclear translocation and/or causing transcriptional inactivation of a subset of GR target genes (41). S134 is unique because the residue is phosphorylated by stress-activating stimuli, and not in a glucocorticoid-dependent manner (42).

1.4.1 Glucocorticoids

Glucocorticoids (GCs) are essential hormones that are produced and released by the adrenal cortex in a circadian manner and in response to stress. The hypothalamic-pituitary-adrenal axis regulates the secretion of these hormones. In a classic negative feedback loop, glucocorticoids also target the hypothalamus and anterior pituitary to inhibit the production and release of corticotropin-releasing hormone and adrenocorticotropic hormone thereby limiting the magnitude and duration of the glucocorticoid increase (39, 42).

There are various kinds of GCs, but they all belong to a class of corticosteroids, and their mechanism of action is onset by stimulating GR (38), which affects metabolism, differentiation, stress responses, immune response, inflammation, cell proliferation, apoptosis and cell survival (1, 43). The importance of synthetic GCs therapeutic regimes is prominent in various medical fields. Synthetic GCs are inexpensive and effectively used to treat inflammatory diseases and hematological malignancies. In breast cancer, it is mainly used as a palliative agent during radiotherapy and chemotherapy to reduce side effects (1, 35). Unfortunately, starting from the early use of GCs, the drug became known for its adverse effects. Hyperglycemia, insulin resistance, diabetes, osteoporosis and muscle waste, just to mention a few, normally emerge during chronic treatment with GCs (43).

Due to the adverse effects, there is a search for safer therapies like alternative (frequently non-steroidal) GR ligands with preserved therapeutic activities, but reduced side effects (43). To improve the therapeutic index, exceeding efforts were initially focused on the development of dissociating GR ligands. The dissociating GR ligands would be capable of downregulating proinflammatory genes but lack the adverse effect of GCs.

Pharmaceutical companies have been bioprospecting and attempting to generate truly dissociating GR activators/modulators called SEGRAM. Currently, SEGRAM has had limited success, and recently, the approach for SEGRAM design shifted towards GR partial agonists following the strategy successfully used for the development of selective modulators of estrogen receptors (SERMs) (43). Generally, the attempt of inventing and further developing these new approaches suggests feasible, improved and safer GR-targeted therapies.

1.4.1.1 Dexamethasone

Treatment with synthetic GCs such as dexamethasone (Dex) is extensively used in cancer therapy. Dex is routinely included in chemotherapy protocols for acute lymphoblastic leukemia, chronic lymphocytic leukemia, multiple myeloma, Hodgkin's and non-Hodgkin's lymphoma (43). In breast cancer patients, Dex is used to help relieve pain, other discomfort and the negative effects caused by chemotherapy (1).

Recent research (1) has observed and concluded that low-dose Dex could reduce tumor growth in MCF7 and MDA-MB-231, and also restrain metastases in MDA-MB-231. High-dose Dex promotes metastases in MDA-MB-231 and tumor growth in MCF7 (1). This indicates that high-dose Dex might not be a sustainable treatment for breast cancer and that low-dose is slightly more favorable(1). GR activation by synthetic GCs such as Dex is not contributing to an optimal treatment for TNBC patients. (1, 40).

1.5 Aim of this thesis

Previously the cell signaling and targeted therapy group at the department of pharmacy, UiT has observed how the cell lines MCF7 and MDA-MB-231 respond differently to certain stress signals and chemotherapeutic drugs on a molecular level. This master thesis aims to continue the comparison of the cell lines and observe their responses regarding the p38 MAPK and GR when stimulated with Ani and Dex. To achieve this, biological assays (proliferation assay, cell viability assay, scratch wound healing assay) and molecular analytic methods (immunofluorescence and WB) were conducted.

2 Materials

Table 1: Breast cancer cell lines

Cell line	American Type Culture Collection (ATCC)	Characteristic
MDA- MB-231	HTB-26	Adherent
MCF7	HTB-22	Adherent

Table 2: Buffers and solutions for cell culture laboratory work

| Product	Producer	Product number
Dulbecco's Phosphate Buffered Saline (PBS)	Sigma Aldrich	D8537
Trypsin – EDTA solution	Sigma –Aldrich	T4049
RMPI - 1640	Sigma – Aldrich	R8758
MEM – Minimum Essential Medium Eagle	Sigma – Aldrich	M4655
Fetal Bovine Serum (FBS)	Biowest	S181B-500
Insulin – solution from bovine pancreas	Sigma – Aldrich	11070-73-8
NuPage® LDS sample buffer	Thermo-fisher scientific	NPOOO8
BOLT ™ Sample reducing agent (10X)	Thermo-fisher scientific	B0009
DAPI	Sigma Aldrich	D9542

Table 3: *Drugs used for stimulating cells*

Product	Producer	Cas number
Anisomycin	Sigma-Aldrich	22862-76-6
Dexamethasone-Water Soluble	Sigma-Aldrich	D2915

Table 4: *Experimental chemicals*

Product	Producer	Cas or Product nr.
Chameleon® Duo pre-stained protein ladder	LI-COR	928-60000
BoltTM 4-12 % Bis-Tris Plus gels (e.g PN: NN04125)	Thermo Fisher Scientific	NN04125
CellTiter-Glo kit	Promega	G9241
Bovine Serum Albumin (BSA)	Sigma-Aldrich	9048-46-8
Prolong Diamond Antifade Mountant (mounting media)	Thermo Fisher Scientific	P36961
4-12 % Bis-Tris Plus gels (10, 12 or 15 wells). (Premade gels)	Thermo Fisher Scientific	NN04125
20X Bolt™ MES SDS Running Buffer	Thermo Fisher Scientific	B000202
Intercept® (PBS) Blocking Buffer	LI-COR	927-60001
DAPI	Sigma-Aldrich	D9542

Table 5: *List of primary and secondary antibodies. If not indicated, the antibody was used for Western blotting. Primary antibodies were stored at -20 ºC and secondary antibodies were stored at 4 ºC*

Product	Manufacture	Product number	Dilution	kDa
α – Actin (rabbit)	Cell signaling	#4968	1:1000	45
GR (mouse)	BD transduction Laboratories	611227	1:4000(WB) 1: 250 (IF)	94
p-P38 (rabbit)	Cell signaling	9211	1:1000(WB) 1: 400 (IF)	43
P38 (rabbit)	Cell signaling	9212	1:1000	40
p-HSP27 (Ser 82) (rabbit)	Cell Signalling	2401S	1:1000	27
p-GR (S134) (rabbit)	Cell signaling	85060	1:1000	91, 94
p-GR (Ser226) (rabbit)	Cell signaling	97285S	1:1000	94, 91
GammaH2Ax (rabbit)	Cell signaling	#2577	1:1000	15
Cyclin D1(rabbit)	Cell Signalling	#2922	1:1000	36
Cyclin D3 (mouse)	Cell Signalling	2936	1:1000	31
Secondary Antibody				
IRDye® 680LT Donkey anti-Rabbit IgG	LI-COR	926-68023	1:20000 /1:15000	
IRDye® 800LT Donkey anti-Rabbit IgG	LI-COR	926-32213	1:20000 /1:15000	
IRDye® 680LT Donkey anti-mouse IgG	LI-COR	926-68022	1:15000	
IRDye® 800CW Goat antiMouse IgG	LI-COR	925-32210	1:15000	
Alexa fluor 568 donkey anti-rabbit	Thermo Fisher Scientific	A10042	1:250 (IF)	
Alexa fluor 488 donkey anti-rabbit	Thermo Fisher Scientific	A-11017	1:250 (IF)	
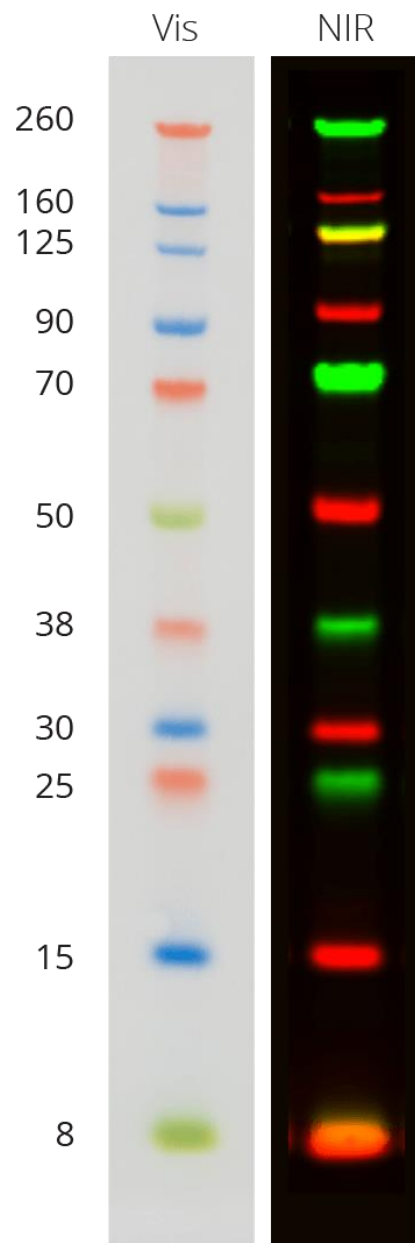
Figure 4: *The Chameleon Pre-stained Protein Ladder was used for proteins detection on western blot. The picture is provided from LI-Cor's homepage and shows multi-colored, pre-stained bands for visual inspection (**Vis**) of the ladder on the blot and two-color near-infrared (**NIR**) detection. The ladder includes 11 protein bands from 8 to 260 kDa.*

Buffers and solutions used in Western Blot

Running buffer

50 ml   Bolt MES SDS Running Buffer (20X)

Fill with dH₂O till 1 l

Blotting buffer

29g   Trisbase

144g   Glycine

1000   methanol

Fill with dH₂O till 5l

TBS (10X)

10g   KCl

400 g   NaCl

200 ml Tris HCl (1 M pH 7,5)

Fill with dH₂O till 5l

TBS – T

500 ml TBS (10X)

5 ml   Tween 20

Fill with *dH₂O till 5l*

Machine and software:

Western Blot

LI-COR Odyssey 9260 Fluorescence Imager

Odyssey Sa Infrared Imaging System

IncuCyte:

IncuCyte2019B Rev2 for handling the machine, detection, and analysis

IncuCyteS3 Live-Cell Analysis System (SARTORIUS)

Immunofluorescence:

ZEN 3.2 (black edition) for handling the microscope, detection

ZEN 3.2 (blue edition) for analysis

LSM 780 Confocal Microscope (Zeiss)

CellTiter Glo:

Reader Control V5.70 R3 for detection

Microsoft Excel (look up the version please) for analysis

CLARIOstar Multimode Microplate Reader (BMG LABTECH) – Luminometer

Software used for figures in results

Excel and Powerpoint, Microsoft version 2202

3   Methods

3.1   Basal cell culture work

Cells were handled in a bio-safety cabinet (Scanlaf MAP safety Class 2 -Labogene). Aseptic techniques were used when cell culture work was conducted. These aseptic techniques involved the use of sterile disposable equipment and cleaning surfaces with ≥70% ethanol to prevent microbial contamination.

3.1.1   Maintaining cell culture

MDA-MB-231 cells were cultured in media containing 90% RPMI and 10% FBS. MCF7 cells was cultured in media containing 90% MEM, 10% FBS and 0,1% insulin. Both cell lines were split twice a week. Cell lines were cultured in Thermo fisher scientific Nunc™ EasYFlask ™ 75 cm^2 (medium) or 175 cm^2 (large) with filter caps. The cell culture flask with cells was labeled with name, cell line, date of splitting and passage number. Cells were stored in a humidified cell incubator (Heracell 150i CO2 Incubator from Thermo fisher scientific) at 37 ºC with 5 % CO_2.

3.1.2   Subculturing cells

Subculturing, also referred to as passaging or splitting cells, is the transfer of some cells from a current culture into fresh growth media. This is a procedure that enables further propagation of the cell line. It is important to split the cells so that the cell culture is not overcrowded. Overcrowding might inhibit the growth of the cells, cause unnecessary deaths because of a decreased access to nutrients and could make cells quiescent.

Procedure: (To split cells)

Cell medium and trypsin EDTA was preheated to 37 ºC in Termaks B8133 Incubator. A Carl Zeiss™ Axio Vert inverted microscope was used to confirm confluency and detect the status of cells. Cells in a medium culture flask were split when cells reached 70 – 90% confluency. In splitting cells, old media was aspirated out of the flask using a sterile autoclaved glass pipette. After aspirating old media, cells were washed with 5 ml PBS by gently swaying it over cells, to wash off remaining media and remove serum. PBS was quickly aspirated and 1,5 mL trypsin

- EDTA was added to cells and the flask was gently tilted around so the solution could cover the cells. Surplus trypsin was aspirated, and the flask was placed in the incubator for 2 – 4 min. Trypsin is a proteolytic enzyme that causes strongly adherent cells to detach from the growth surface in the flask. This method is fast and reliable but can damage the cell surface by digesting exposed cell surface proteins, so the process was monitored by looking at the cells in the microscope. When cells had detached 10 mL of preheated media with serum was added to cells to neutralize the effect of trypsin – EDTA. Carefully pipetting up and down in the flask, flushing the surface where the cells had attached, was done to optimize the detaching and dispersion process. The cells were now ready to be counted and seeded (if they should be used for experiments), or they were directly passaged (split) to fresh media. For maintaining cells for further passages, the split ratio for MDA MB 231 cells were 1:10, and MCF cells were 1:3. After transfer of the appropriate volume of cells to a flask, additional media was added giving a total volume of about. 10 mL per 75 cm^2 culture flask.

3.1.3 Counting cells and seeding cells

Cell suspensions of 10 µL were directly pipetted into the chamber of the DeNovix CellDrop™ FL fluorescence cell counter. With the brightfield application, cells were automatically counted as x amount of cells/ml. After counting, cells were wiped away with lens paper.

Seeding cells is an act of spreading a certain number of cells to an appropriate cell culture vessel to be able to perform experiments. After trypsinization as described above, cells were counted and seeded in appropriate wells. In the succeeding experiments cells were seeded in Falcon 6 - , 12, and 96 well plates according to appropriate confluency.

After seeding cells, the well plate was tilted from side to side, whilst avoiding a rotational motion, so the cells could spread evenly in the media and not just end up in the middle. After seeding cells, the plates were placed in the incubator at 37 ℃ with 5% CO_2 overnight before stimulation or other experiments were performed.

3.2 Experimental cell culture work

3.2.1 Stimulating cells

For experiments involving stimulation with drugs, the cells were seeded and left overnight in the incubator. The next morning the media was aspirated, and new fresh media containing the desired concentration of drug was added. The cells were placed in the incubator and harvested at specific time points (e.g. 30 min or 24 hrs after stimulation), for Western blot analyses, or placed in the IncuCyte machine and monitored there for up to e.g. 3 or 7 days, depending on the experiment.

Anisomycin (Ani) and Dexamethasone (Dex) in different concentrations were used as the main stimulants for the two cell lines throughout the experiments. Dex stock was 1mM, (solid Dex powder mixed in water). The Dex solution was covered in aluminum foil and stored at 4 ℃. A novel stock solution was made every 2 weeks. Dilutions of the Dex stock solution were made in an appropriate media and distributed on the cells so that the final concentrations were between 1 and 200 nM. The Ani stock (10mg/ml) was stored at -20 ℃ in aliquots and thawed each time before being diluted with appropriate media. Dilutions made of stock and mixed with appropriate media were freshly made for each experiment.

3.2.2 Anisomycin titration

For this experiment, each cell line was seeded 250 000 cells/ well in a 6 well plate with 2 ml media per well and left-over night in the incubator. The next morning the cell media was replaced with fresh media containing different drug concentrations. The stock solution of Ani is 10 mg/ml. From stock, a 1:100 dilution = 0,1 µg/µl was made in media, and from this, the remaining dilutions were made. Dilutions of Ani used were 0,1 µg/ml, 1 µg/ml, 5 µg/ml, 10 µg/ml and 20 µg/ml. Non-treated cells were used as control. Cells were lysed after 30 minutes and used in WB as described in title 3.6 (Results in Figure 6)

3.2.3 Dexamethasone titration

Each cell line was seeded 250 000 cells/ well in a 6 well plate with 2 ml media per well, incubated at 37 ℃ with 5% CO_2 overnight. The next morning the media was aspirated, and 1 ml of fresh media was added per well. Cells were stimulated with Dex (1nM, 10nM, 50nM, 100nM, 200nM) and left in the incubator for 30 min before cell lysis. Non-treated cells were used as control. Lysates were analyzed with WB as described in 3.6. (Results in Figure 8)

3.2.4 Anisomycin time study

Each cell line was seeded 250 000 cells/ well in a 6 well plate with 2 ml media per well, incubated at 37 ℃ with 5% CO_2 overnight. After incubation, old media was aspirated and added 1 ml of new fresh media per well. All cells were stimulated with 0,1 µg /ml Ani. Non-treated cells were used as control. Cells were incubated for (5 min, 10 min, 15 min, 20 min and 30 min before cell lysis. Lysates were analyzed with WB as described in title 3.6 (Results in Figure 8)

3.2.5 DNA damage detection

3.2.6 Induction of DNA damage by UV irradiation

Each cell line was seeded 300 000 cells/well on three 6 well plates with 2 ml media per well, incubated at 37 ℃ with 5% CO_2 overnight. One 6 well plate was used as control and was not exposed to UV light but in RT when removed from the incubator for the same time as the cells treated with UV light for 10 minutes and 30 min. The two remaining plates were exposed to UV light for either 10- or 30-min UV transilluminator (UVP) on maximum strength. After UV irradiation, the cells were re-incubated at 37 ℃ with 5% CO_2. for 2 h before cell lysis with lysis buffer and analyzed via WB as described in title 3.6 (a part of the results in Figure 16)

3.2.7 Cell recovery study

To study cell recovery the cells were initially stimulated with the drugs for 24 hrs before the drugs were replaced with fresh media and the proliferation was continuously monitored for 3 more days in IncuCyte. In two 6 well plates 150 000 cells/ well were seeded with 2 ml media

per well and incubated at 37 ℃ with 5% CO_2 overnight. The plates should be treated similarly with regard to the drugs. One of the plates was for monitoring the proliferation in IncuCyte after stimulation (recovery cells), whilst the second plate would be harvested before recovery to illustrate the effect the drugs had on the cells after 24 hrs (control cells).

After the overnight incubation media was aspirated and cells on each plate were stimulated: with either 0,1 µg/ml Ani or 50nM Dex. Non-treated cells were used as control. One of the plates was placed in the incubator, and here the cells were lysed and harvested for WB after 24 hrs. The other plate was placed in the IncuCyte, and after 24 hrs the media containing drugs were removed and 2 mL of fresh media was added to each well. The plate with recovery cells was placed back into IncuCyte for an additional 3 days before cells were lysed and harvested for WB. Proliferation was analyzed by use of IncuCyte and changes in proteins or protein modifications were analyzed by WB as described in title 3.6. (Results in Figure 15 and Figure 16)

3.3 Proliferation assay

Table 6: Amount of cells seeded for the monitorization of cell proliferation in MDA-MB-231 and MCF7 breast cancer cell lines with IncuCyte.

MDA-MB-231		MCF7	
Well	Amount of cells	Well	Amount of cells
1	1000	7	1000
2	2000	8	2000
3	3000	9	3000
4	4000	10	4000
5	5000	11	5000
6	6000	12	6000

Cells were seeded in a 12-well plate according to Table 6 with 1 ml media per well. After incubation at 37 ℃ with 5% CO_2 overnight, the plates were placed in IncuCyte for 7 days to

monitor growth, cell health and morphology. 3 pictures from each well were taken every 3 h. This gave a natural proliferation status of the cells. (Results in Figure 10)

The IncuCyte(sartorius) is a live-cell imaging and analysis platform that provides quantification of cell behavior over time. The Incucyte's ability to continuously collect and analyze images from live cells in an incubator over time gives the opportunity to efficiently capture cellular changes in real-time. Proliferation assays and migration assays have been conducted using Incucyte.

3.3.1 Anisomycin and Dexamethasone stimulation

MCF7 cells: Seeded 150 000 MCF7 cells/ well in two 6 well plates with 2 ml media per well, incubated at 37 ºC with 5% CO_2 overnight. After incubation, old media was removed and 1 ml of new fresh media was added to each well. Cells were stimulated with Ani (0,1 µg/ml, 10 µg/ml) and Dex (50nM, 100nM) and unstimulated cells were used as control. The two 6 well plates were directly placed in IncuCyte for monitoring. 3 pictures from each well were taken every 3 hrs. After 3 days, 1 ml fresh media containing the same drug concentration was provided for each well, and the incubation in IncuCyte continued for an additional ca. 3 days. The cells were then subjected to lysis buffer and prepared for WB.

MDA MB – 231 cells: Same procedure as described for MCF7 cells above, but cells were harvested for WB after 3 days. (Results in Figure 11 and Figure 12)

3.3.2 Cell viability assay

The CellTiter-Glo cell viability is a luminescence-based assay that quantitatively detects live cells based on metabolic activity, measured as adenosine triphosphate (ATP) levels. A Luminometer (BMG LABTECH) is used to measure the amount of light produced in each sample due to the ATP. Measurements of the signal are expressed as relative light units (RLU).

Each cell line was seeded 150 000 MCF7 cells/ well in a 6 well plate with 2 ml media per well, incubated at 37 ºC with 5% CO_2 overnight. After incubation, used media was aspirated and 1 ml of new fresh media was filled in each well. Cells were stimulated for 30 minutes with Ani (0,1 µg /ml, 10 µg/ml) and Dex (50nM, 100nM), starved cells were included (media without

FBS and insulin). After stimulation, media was aspirated from all wells, and 300 µl fresh new media + 300 µl CellTiter-Glo reagent was pipetted into each well, resulting in 600 µl CellTiter-Glo suspension/ well. The well plate was covered with aluminum foil and placed on a shaker for 10 – 15 min, so the cells could lyse. After cell lysis, samples from the 6 well plate were transferred to a white opaque 96 well plate and covered with aluminum. Samples in the opaque 96 were analyzed by a luminometer. This experiment was done again, but with a 24h stimulation time. (Results in Figure 13)

3.4 Migration assay

Scratch wound assay is a convenient method to study the migration of cells *in vitro*. An artificial wound is made by making a scratch in a confluent cell culture, and the cells recovery (migration into the wound area) is monitored over time by IncuCyte.

Each cell line was seeded 60 000 cells/ well in a 96 well plate with 100 µl cell suspension per well. Cells were incubated overnight. After incubation, a WoundMaker™ from the IncuCyte Cell Migration Kit was used to create a scratch wound in each well. Old media was aspirated before new media with or without drugs were added. Cells were treated with Ani (0,1µg /ml, 10 µg/ml) and Dex (50nM, 100nM). Non-treated cells were used as control. Each well contained 100 µl. Cell migration was monitored and analyzed by use of IncuCyte with 1 picture from each well taken every hr. MDA-MB-231 cells were left for 24 h, while MCF-7 cells were left for 5 days. On day 3 fresh media containing the same drug concentration was added to the MCF7 cells on top of the existing media, increasing the total volume to 200 µL media/ well. (Results in Figure 14)

3.5 Immunofluorescence

Immunofluorescence (IF) is a method in biology that uses antibodies chemically labeled with fluorescent dyes to visualize molecules under a light microscope. In a 12-well plate, MCF7 cells were seeded 60 000 cells/ well and MDA-MB-231 cells were seeded 50 000 cells/ well with 1 ml media per well. In a 24-well plate, each cell line was seeded with 30 000 cells/ well with 500 µl media per well. Cells were seeded on sterile glass coverslips in the wells and incubated overnight. After incubation, old media was aspirated, and cells were treated with 0,1

µg/ml Ani and 50nM Dex for 1h. Non-treated cells were used as control. Media was then aspirated, and cells were washed once with PBS, then fixed with ice-cold 100% methanol for 10 min in the freezer (-20 ℃). After fixation, cells were washed twice with PBS.

For immunostaining, PBS was removed from the fixed cells at the coverslips and 1% BSA in PBS was added and incubated for 30 min in RT. Cells were washed once with PBS. An appropriate volume of primary antibody/ antibodies diluted in 1% BSA in PBS was directly put on coverslips and incubated for 1 h at 37 ℃. After incubation, cells were quickly washed with PBS, then washed twice with PBS (10min x 2 times on a shaker), and lastly washed with 1% BSA in PBS on a shaker for 10min in RT.

From here on all processes were performed in darkness. The secondary antibodies were applied directly onto the coverslips and incubated for 1 h at 37 ℃. 200 µl DAPI (Hoechst 1:2000 in PBS) solution was applied on coverslips and incubated for 10 min in RT. DAPI and secondary antibody aspirated and coverslips were swayed once with PBS, then washed twice with PBS (10min x 2times on Stuart Scientific Platform Rocker STR6) and lastly washed with 1% BSA in PBS for 10min on a platform rocker. Coverslips with cells facing downwards on microscope slides were mounted with small drops of mounting media and incubated at RT overnight in the dark. Fluorescent microscopy images were obtained using a fluorescence microscope system - Zeiss Confocal Microscope (Zeiss), and pictures were taken using the ZEN 3.2 (black and blue Microscope slides were stored at 4 ℃, when not in use. (Results in Figure 9)

3.6 Western blot

SDS-PAGE is the step before WB and is an electrophoresis method that separates proteins according to their MW, and this method was achieved using premade gels. Western Blot (WB) is an analytic technique that is used to detect specific proteins in cell extracts. Allowing the proteins to a membrane so they can be detected by specific antibodies.

3.6.1 Harvesting cells for WB

Cells were harvested for Western blot via cell lysis. The lysis buffer consists of 450 µl NuPage® LDS Lysis buffer and 180 µl BOLT ™ Sample reducing agent (10X)

After stimulating cells for the appropriate time in 6- or 12 well plates, the plate was taken out of the incubator and the rest of the procedure was performed in non-aseptic conditions. Media was aspirated from the well, and cells were washed with 1 – 2 ml PBS. PBS was completely removed before lysis buffer was added because residual PBS would have changed the total volume of the lysis buffer and thus changed the comparable amount of cells loaded on the gel. Eighty µl lysis buffer was used for each well in 12 well plates, whereas 80 or 100 µl were used for 6 well plates. A cell scraper was quickly used to detach cells., That the cell lysis mixture became more viscous was a sign that cell lysis had worked and that the lysate contained DNA. The cell lysis mixture was pipetted into a labeled Eppendorf tube and placed in an ice bath till the next step.

Eppendorf tubes were placed in a Stuart Dual Control Digital 2-Block Heater at 100 degrees for 5 – 8 min and then placed back in the ice bath. To truncate/cut DNA strands and make the samples less viscous, the samples were sonicated with Diagenod's Bioruptor® UCD-200 in cold water (ice water) for 5 minutes, with alternating cycles of 30 sec on and 30 sec off. After sonication, cells were centrifuged on maximum speed in Heraeus Biofuge PICO 21 for 2 min to get rid of insoluble cell debris. Cell - lysates samples were kept on ice and analyzed via WB Remaining lysates were stored in cardboard cryo-boxes in the freezer (– 20 ℃).

3.6.2 SDS-PAGE

Premade gels were made Bolt^{TM} 4-12 % Bis-Tris Plus gels have a suitable number of wells (10, 12 or 15). The combs were removed and the wells were washed 2 – 3 times with MES SDS running buffer (diluted 1:20 from a 20X stock with RO water). After washing the wells, the white stripe on the bottom of the gel was removed to provide a connection between the buffer chambers allowing electric current to pass through the gel. The gel was mounted in the Bolt™ Mini Gel Tank with cassette clamps. On one side of the gel, the tank was filled with running buffer until the wells on the gel were completely covered with running buffer. On the other side of the gel, the tank was filled with running buffer until half full.

Three µl chameleon duo MW marker was pipetted in one of the first wells. Then 10 µl of lysate sample was pipetted per well. The mini gel tank lid was placed on top of Bolt™ Mini Gel Tank and the wires on the lid were connected to a power supply (PowerEase 500, Thermo Fischer Scientific). The gel was run for 45 or 30 min with a constant voltage of 200V. Whilst the gel

was running, preparations for the blotting procedure were started. Odyssey nitrocellulose membrane (name of product and company is needed) was cut into a square of 7,5 x 7 cm and marked with a pencil on the edge to identify the blot. Labeled membrane, blotting sponge pads and filter papers were pre-soaked in the blotting buffer.

When the running of gel was completed. The membrane was placed with the correct side facing the gel and assembled with the sponge pads and filter papers as illustrated in Figure 5. The blot sandwich was made in a mini blot module consisting of a cathode core and an anode core. From cathode to anode the blot sandwich has an order of assembly that consists of a sponge pad, filter paper, SDS-PAGE gel, membrane, filter paper and sponge pad.
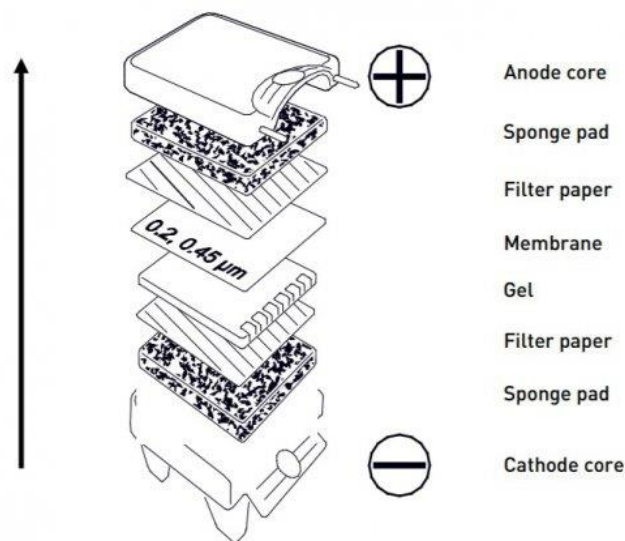

Figure 5: Order assembly of a blot sandwich. Figure taken from Thermo-fisher scientific western blot protocol

A blot roller was used to remove any trapped air bubbles in the sandwich. The sandwich was then cushioned together in the blot module and placed tightly in the tank, and the tank was filled with RO water. Blotting was run for 1 or 2 hrs, depending on the size of the proteins to be detected, and the current was constant at 160Am. This process allows the protein to move from the gel and onto the membrane, so the proteins can be detected by antibodies. A successful protein transfer is confirmed when the chameleon duo pre-stained marker is visible on the nitrocellulose membrane after blotting.

After blotting, the membrane was placed in a 50ml falcon tube and 3 mL Intercept® (TBS) Blocking Buffer was added and placed on a tube rotator in RT for about 1 h. The blocking buffer reduces background interference and improves the signal-to-noise ratio thereby

increasing the sensitivity of the assay. The blocking buffer was replaced by a primary antibody appropriately diluted in the blocking buffer containing 0,1% tween 20. For the applied dilution of individual antibodies see Table 5. The tube was then placed at 4 C on a Stuart roller mixer STRT1 overnight. The next day the membrane was turned and washed with TBS-T in the falcon tube for 10 min, so the membrane will not be curled. After washing, the membrane became flat and was then placed in a Li-cor box and washed for 5 minutes 4 times with TBS-T. A secondary antibody (Table 5) was diluted in TBS-T added and the membrane was incubated on a Stuart Scientific Platform Rocker STR6 for 1 hr in RT. The membrane was then washed with TBS- T 4 times 5 min and developed using the Li-Cor Odyssey Sa Infrared Imaging system. Blots were stored covered in TBS-T at 4 ºC or dried and stored in clear plastic sleeves in a ring binder. Dry membranes need to be soaked in TBS-T for about 1 hr before they can be stained again.

4 Results

While targeted therapy exists for ER-positive breast cancers, the treatment option for TNBC is conventional chemotherapy giving a poorer prognosis. It is therefore of interest to study molecular mechanisms and differences between these two cell lines. The MCF7 and MDA-MB-231 cell lines are frequently used for breast cancer research. These cell lines are in vitro representative models for luminal A (non-aggressive) and basal-like (aggressive) breast tumors (8). MCF7 is ER and PR positive, while MDA-MB-231 (TNBC) is lacking ER, PR and HER2.

GR is expressed in all cells, and since treatment with the synthetic glucocorticoid dexamethasone (Dex) is standard for BC patients, any difference in GR activity between ER+ and TNBC as a response to chemotherapeutic treatment could be worth following up in regard to the development of targeted therapy. In this master thesis, it was of interest to do further investigations to look for differences, both at the molecular and functional level, after stimulation with Ani and Dex. MCF7 and MDA-MB-231 were chosen as model cell lines for ER-positive and TNBC respectively. WB was used to study the molecular responses to the stimuli, while proliferation, cell viability and migration assays were done to study the functional responses.

4.1 Anisomycin - a potent and rapid p38 – MAPK activator in MCF7 and MDA-MB-231 cells

Initial observations had been done with 10 µg/ml Ani, and previous studies have detected biological effects of Ani at concentrations below 10 µg/mL (35, 36). It was of interest to examine if lower concentrations than 10 µg/ml of Ani could activate the p38 MAPK signaling pathway and affect GR phosphorylation. Therefore, a titration study was performed where each cell line was stimulated with different concentrations of Ani 0,1 µg/ml, 1 µg/ml, 5 µg/ml, 10 µg/ml and 20 µg/ml and non-treated cells were used as control. Cells were lysate after 30 minutes and used and analyzed by WB. It was decided that 0.1 µg/ml (new concentration) and 10 µg/ml (initial concentration) Ani should be used for further experiments, to compare their effects on the cell lines. Antibodies against phosphorylated (p-p38) and unphosphorylated p38 MAPK (p38) were used to identify the amount of activated p38 and the total amount of p38, respectively. Actin was used as a loading control.

For both MCF7 and MDA-MB-231 cells activated p38 is observed with the lowest concentration of Ani (0.1 µg/ml) (Figure 6). Whereas the activation of p38 does not change with increasing concentrations for MDA-MB-231 it seems to decrease with increasing concentrations for the MCF7 cells. However, since the Actin staining also seems to be somewhat decreased for the higher concentrations in MCF7 it could also be a matter of decreased protein loading on the gel. GR is known to be decreased on WB upon ligand binding and activation (44) and several sites are known to be phosphorylated as a response to different signalling pathways. Serine-226 (S226) is reported to be phosphorylated by JNK upon stress signaling (45) and Serine-134 (S134) is reported to be phosphorylated by activated p38 (40, 45) For both cell lines, it is observed that S134 is phosphorylated after stimuli with the lowest Ani concentration (Figure 6). For MCF7 all concentrations of Ani seem to give approximately the same effect on the S134 phosphorylation, whereas for MDA-MB-231 cells the effect appears to be strongest for the 1µg/ml concentration. There was no background phosphorylation observed for S134 in the unstimulated cells, whereas phosphorylated S226 could be observed also in unstimulated cells for both cell types. The pattern of phosphorylated S226 did not seem to change according to Ani stimulation in the MCF7 cells (Figure 6), but for MDA-MB-231 cells, the phosphorylated S226 staining seemed to decrease with the highest concentrations of Ani (Figure 6). It is clearly shown in both

cancer cell lines, that Ani causes signal transduction through the p38 MAPK, and its activation is important for the phosphorylation of the S134 residue on GR.
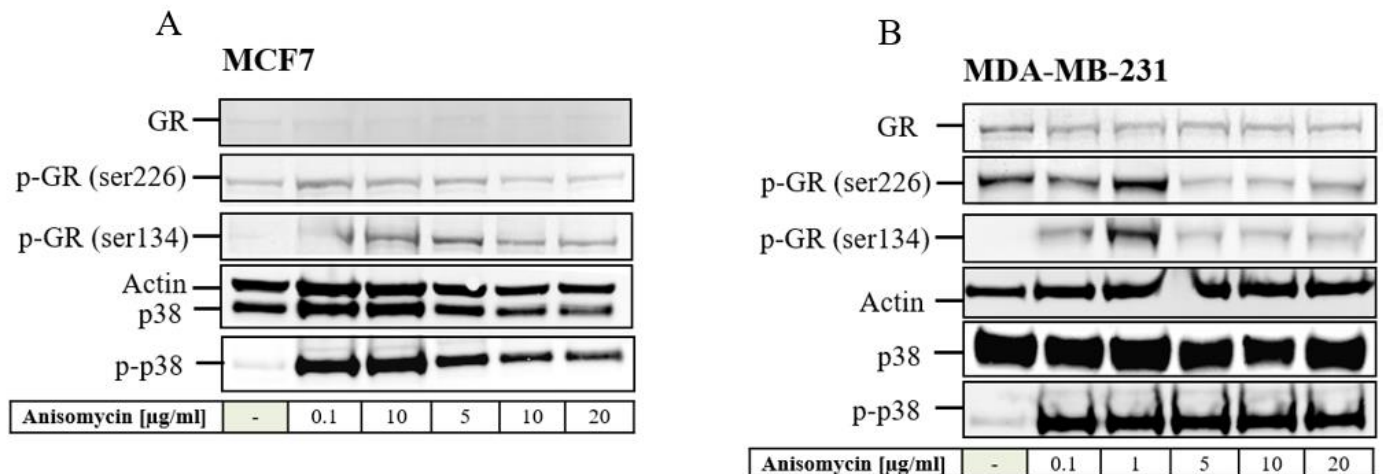

Figure 6 A titration study of Anisomycin shows that 0,1 µg/ml is sufficient to activate p38 and cause GR S134 phosphorylation in MCF7 and MDA-MB-231 cells. *Each cell line was stimulated with Anisomycin: 0,1 µg/ml, 5 µg/ml, 10 µg/ml and 20 µg/ml. Cells were stimulated for 30 minutes before cell lysis. Non-treated cells were used as control. Cell lysates were analyzed by Western Blot. Antibodies used are displayed in the figure. Actin was used as a loading control*

In the Ani titration study, cells were incubated for 30 min. It was also of interest to examine how rapid the activation of p38 would occur. Each cell line was stimulated with 0,1 µg /ml Ani. Cells were incubated for (5 min, 10 min, 15 min, 20 min, and 30 min) before the cells were subjected to lysis buffer and prepared for WB. The WB for both cell lines shows activation of p38 as early as 5 minutes after Ani stimulation (Figure 7A and B), and the intensity of the activation only increases slightly at 10 and 15 min, and then is kept at the same level at 20 and 30 minutes. These results reveal that Ani is a potent drug that has a rapid effect on the activation of the p38 MAPK in both cell lines.
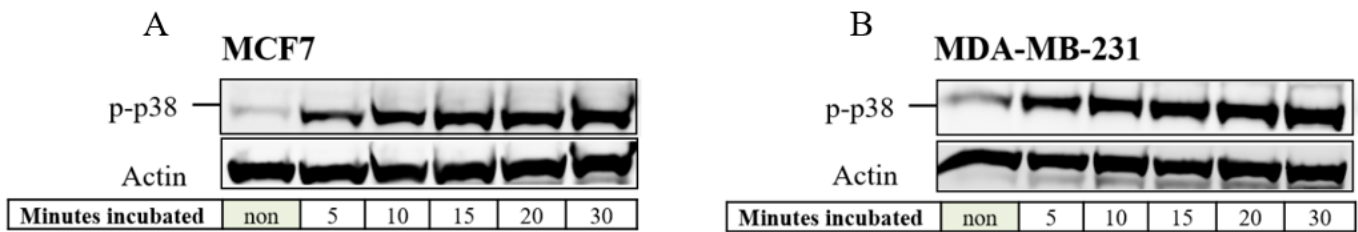
Figure 7: A time study of Anisomycin shows that 0,1 µg/ml Anisomycin activates p38 in MCF7 and MDA-MB-231 after 5 minutes incubation. Cell Lysates from MCF7 and MDA-MB-231 cells after time study titration. Each cell line was stimulated with 0,1 µg/mL and incubated for 5, 10, 15, 20 and 30 minutes before cells were subjected to lysis buffer and prepared for WB. Non-treated cells were used as control. Cell lysates were analyzed by Western Blot. Antibodies used are displayed in the figure. Actin was used as loading control

4.2 Dex treatment results in molecular differences in GR between MCF7 and MDA-MB-231

GR has been identified as one of the downstream targets in the p38, and observations show that the phosphorylation of S134 on GR is dependent on the p38 MAPK signalling pathway (45, 46). Dex was also examined in this study to observe if ordinary activation of GR by a GC ligand also would be different in these cell lines A Dex concentration of 100 nM has been used successfully for several cell lines to activate GR. Here we tested concentrations of 1, 10, 50, 100 and 200 nM for the two breast cancer cell lines. The cells were stimulated for 30 min and then subjected to lysis buffer and prepared for WB. Non-treated cells were used as control. It was decided that 50 nM(new concentration) and 100 nM Dex (initial concentration) both should be used for further experiments. We and others have shown that a p38 MAPK activation leads to the ligand-independent phosphorylation of S134 on GR (40, 45). Since it is shown in Figure 6 that the kinetics of this GR phosphorylation is different between the MCF7 and MDA-MB-231, it was of interest to see if an ordinary GR activation by a GC ligand would be different between the two cell lines. Increasing concentrations of Dex seem to decrease GR expression in MCF7 cells, with no detection of GR at the two highest concentrations (Figure 8A). Since GR detection on WB is known to be decreased after

Dex stimulation (44), the observed reduction in GR for MCF7 cells most likely indicates that GR is ligand-bound and activated. However, for MDA-MB-321 cells a decrease in GR expression upon Dex stimulation is not clear (Figure 8B). A slight decrease in GR can be observed for the 3 highest concentrations of Dex, but so is Actin. and it could therefore be a matter of decreased protein loading on the gel. An interesting difference was also observed for the S226 activation. For MCF7 one can see that p-GR S226 is only increased at concentrations of 1 nM and 10 nM Dex. MDA-MB-231 non-treated and treated cells show p-GR S226 regardless of GCs ligand binding, but p-GR S226 seems to decrease upon higher concentrations. In addition, there seems to be a weak background staining for p-GR S134 in MDA-MB-231, which might increase with the lowest concentrations of Dex, but not with the highest (Figure 8B). For MCF7 cells the S134 phosphorylation of GR is not affected by Dex stimulation. There were clear differences in MCF7 and MDA-MB-231 upon ligand-dependent GR activation. MCF7 showed a more prominent activation of GR, because there were no signals of GR in MCF7 upon higher concentrations of Dex compared to MDA-MB-231. Residual p-GR S134 was not dependent on GCs ligand depended on activation.
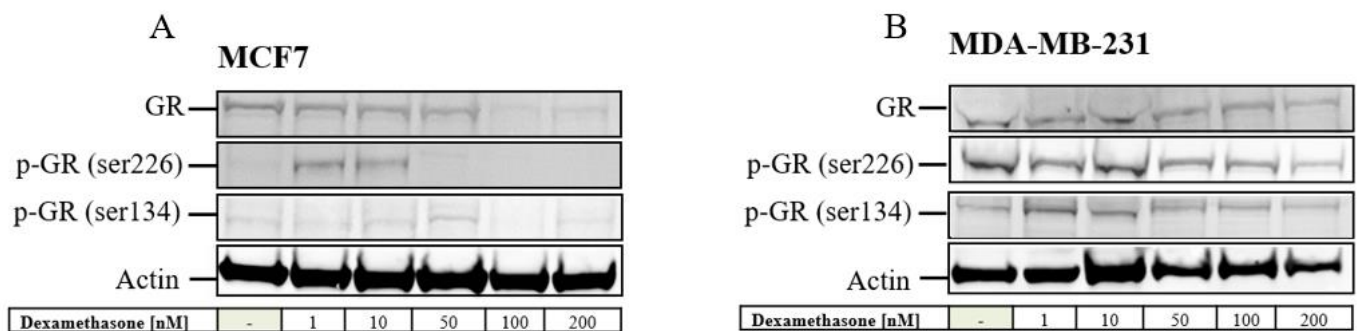

Figure 8: A titration study of dexamethasone shows that there is a difference in the cell lines upon activation of dexamethasone concentrations ≥50nM. Each cell line was stimulated with different concentration of Dex (1 nM, 10 nM, 50 nM, 100 nM and 200nM) in 30 minutes before cell lysis. Non-treated cells were used as control. Cell lysates were analyzed by Western Blot. Antibodies used are displayed in the figure.

4.3 Localizing p-p38 and GR in Ani and Dex treatment

GR is normally localized in the cytosol and translocated to the nucleus upon ligand binding (40). This translocation is essential for its function as a transcription factor. Whereas it is well known that Dex promotes such a translocation, less is known about the effect of ligand-independent S134 phosphorylation caused by activated p38(40).

p38 is also primarily in the cytosol, but upon phosphorylation and activation some p38 can also be found in the nucleus, and it is known to translocate in and out of the nucleus (47, 48). It was therefore of interest to also look at the localization of activated p38 (p-p38) after stimulation with Ani and Dex in both cell lines. Fixed cells were stained with antibodies for GR and p-p38 and pictures were taken by use of a confocal microscope (Figure 9). To examine the localization of GR both cell lines were treated with low dose Ani (0,1 µg/ml) and Dex (50 nM) for 1 hr before they were fixed and prepared for immunofluorescence (IF).

In non-treated cells, the GR is mainly localized in the cytoplasm for both cell types. However, for some of the MDA-MB-231 cells, GR is observed in the nucleus even in the non-treated cells. This was not observed for MCF7 (Figure 9). However, Ani treated MDA-MB-231 cells seem to lose their intense GR expression in cytosol compared to non-treated cells. There is no difference between Ani-treated and non-treated MCF7 cells. Non-treated MDA-MB-231 had a strong GR expression in the cytosol. After Dex treatment, the expression of GR has increased as expected in the nucleus, however, the translocation is not complete and there is still some GR in the cytosol (Figure 9). MCF7 also gets increased GR in the nucleus after stimulation with 50 nM Dex, but the translocation is not as efficient as for the MDA-MB-231 cells, and most GR remains in the cytosol. To summarise, MDA-MB-231 generally has an increased basal level of GR in the nucleus in unstimulated cells compared to MCF-7 and also shows more efficiency in translocation of GR to the nucleus after stimulation with Dex.

Unfortunately, the quality of the p-p38 staining was not good compared to the GR staining, so it was difficult to detect p-p38, especially in the anisomycin-treated cells. We would have expected an equally increase expression of p-p38 in MCF7 and MDA-MB-231 (Figure 9).
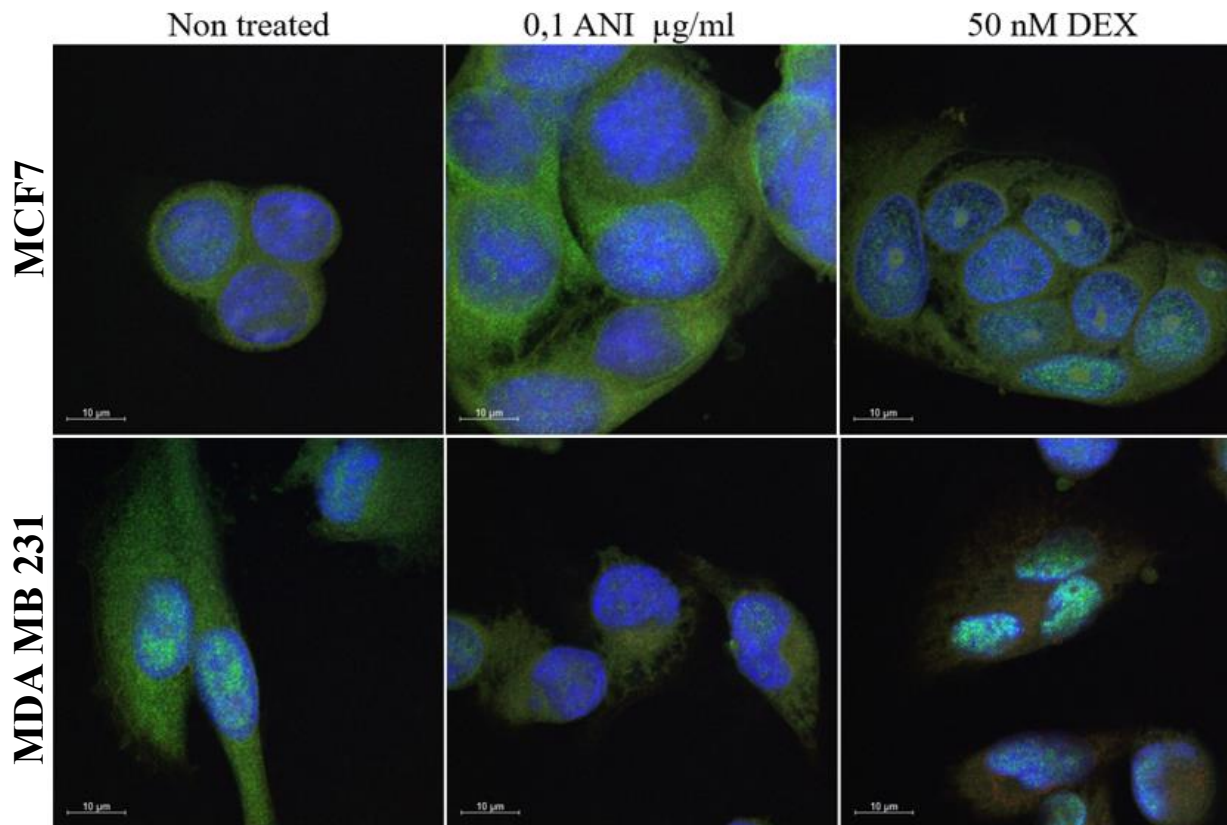
Figure 9: The expression of GR is different in MCF7 and MDA-MB-231. *Each cell line was stimulated with 0,1 µg/ml Ani and 50 nM Dex for 30 min, before fixated and detected by immunofluorescence. Non treated cells were used as control. Cells were stained with Antibodies p-p38 (Alexa 568) and GR (Alexa 488). DAPI (in blue) was used for visualization of the nuclei.*

4.4 Effects of Anisomycin and Dexamethason on MCF7 and MDA-MB-231 cells proliferation, cell viability and migration

To determine the biological effects of Ani and Dex on the cell lines, a proliferation assay, cell viability assay and migration assay were performed. p38 MAPK activity regulates cell survival but can enhance migration in cancer cells. (47). High and low concentrations of Ani are both shown to cause molecular responses for p38 activation and GR phosphorylation of-S134. The two concentrations of Dex were being in the borderline for molecular effects shown on GR in MCF7 was used.

4.4.1 Baseline cell proliferation

Changes in the proliferation rate for the cells will be monitored to see what effect the different drugs will have on each cell line. Therefore, the first thing to do was to observe the proliferation rate of the two cell lines without any stimuli and determine at which density the cells should be seeded for the proliferation experiments. Each cell line was seeded in 6 different concentrations ranging from 1000 to 6000 cells per well and monitored in the IncuCyte for 7 days. The proliferation rate accelerated after 3 days for both cell lines (Figure 10). MDA-MB-231 cells had an increased proliferation rate according to confluency compared to MCF7 cells (Figure 10). The MDA-MB-231 cells also had a proliferation rate that was proportional to the number of cells that were seeded in the well (Figure 10).
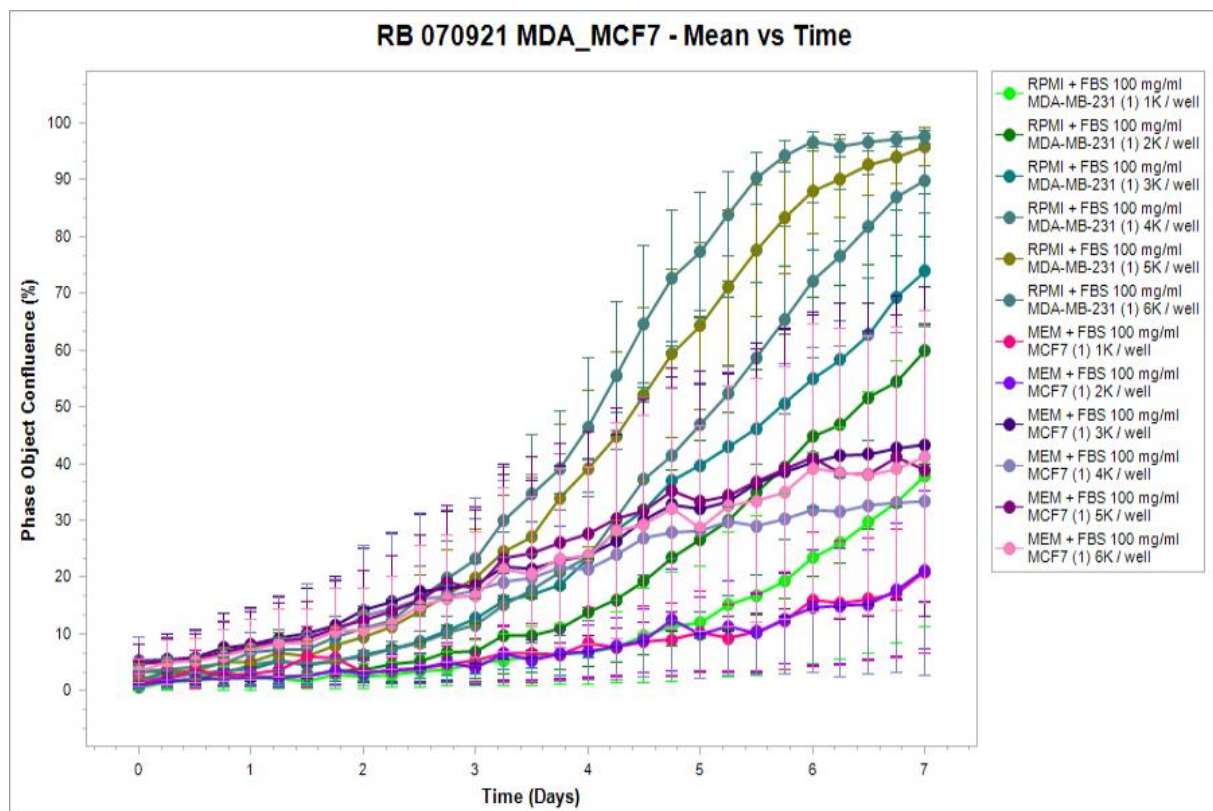

Figure 10: MCF7 and MDA-MB-231 cells show different rates of proliferation when monitored in IncuCyte for 7 days. *Each cell line was seeded in 6 concentrations ranging from 1000-6000 cells per well in a 12 well plate and left for monitoring in IncuCyte for 7 days. Cells were not stimulated and remained in the same media whilst being monitored in the Incucyte.*

4.4.2 Anisomycin treatment

In Figure 11, there is no proof of decreased protein expression. But the decrease in actin (and p38 and GR) show that there is a general decrease in proteins in these lysates, which could indicate that the cells are dead, especially at 10 µg/mL. To detect the proliferation each cell line was stimulated with Ani (0,1 µg/ml, 10 µg/ml) and Dex (50nM, 100nM) placed in IncuCyte for monitorization. 3 pictures from each well were taken every 3 hr. MCF7 cells were in IncuCyte for ca. 6 days and new media with stimulation was added after day 3 mixed with old media. MDA-MB-231 cells were in IncuCyte for 3 days. After IncuCyte the cells were then subjected to lysis buffer and prepared for WB.

It was notable that proliferation was inhibited in Ani-treated cells (Figure 11A and B). Observing all the antibody staining, especially the phosphorylated GR, there is no proof of decreased phosphorylation signals (Figure 11). But the decrease in actin, p38 and GR show that there is a general decrease in proteins in these lysates, which could indicate that cells are dead or less viable compared to non-treated cells. The WB of the cell lysates from the proliferation assay shows that the protein expression in the cell decreases in a dose-dependent order to ani stimulation (Figure 11C and D).

Observations indicate that there might be a difference in the p38 activity between the cell lines, upon prolonged Ani treatment. There was a detectable difference in p-p38 between the cells at the end of the proliferation experiment. Notably, for both cell lines p-p38 staining was detected in non-treated cells, indicating that the incubation conditions during the proliferation experiment probably have activated the p38 MAPK pathway. However, for the 0.1 µg /ml Ani treated cells, the p38 pathway is activated in MDA-MB-231 cells (Figure 11D) while p-p38 is hardly detected in MCF7 cells (Figure 11C). In addition, it might seem that the expression level of p38 in MCF7 cells is more affected (decreased) upon Ani stimulation than it is in the MDA-MB-231 cells when comparing non-stimulated and 0.1 µg/ml stimulated lysates (compare Figure 11C and D) In this study, it might be the prolonged incubation time for MCF7 that influenced the results, but it seems that both the activation and expression of p38 in this cell line are decreased compared to MDA-MB-231. MCF7 has an increased pHSP27 in its non-treated cells, and the MDA-MB-231 cells do not have the expression of pHSP27. HSP27 is a downstream substrate of p38 MAPK. (Figure 11C and D). And this indicates that activation of the p38 MAPK results into different molecular results.
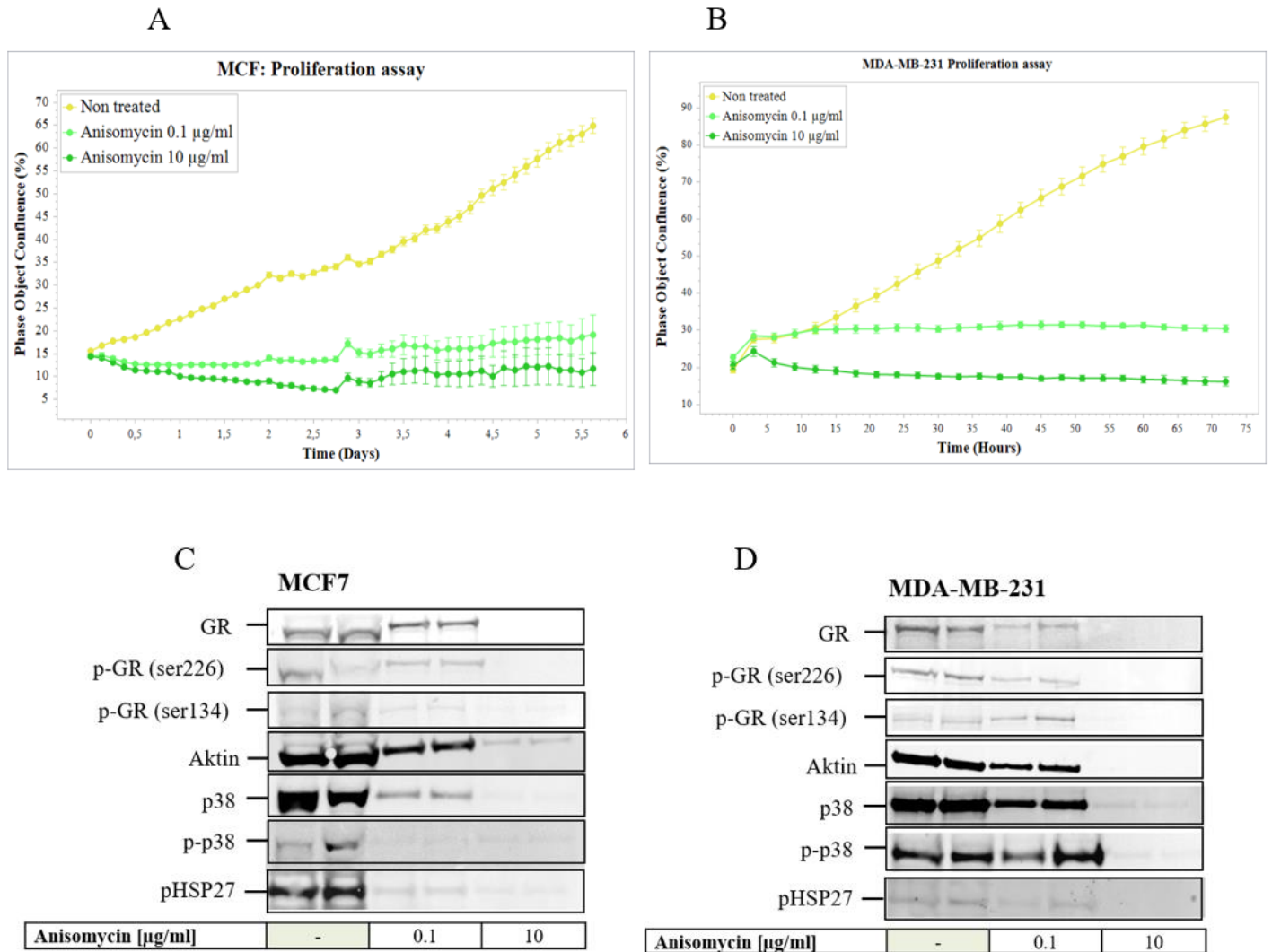
Figure 11: Ani stimulations inhibited the proliferation in both cell lines. *Each cell line was stimulated with 0,1 µg/mL and 10 µg/mL Ani, then placed in IncuCyte and monitored according to their confluency. Cells from the proliferation assay were subjected to lysis buffer and prepared for WB. Non-treated cells were used as control.* ***A)*** *proliferation assays of MCF7, cells were incubated in IncuCyte for 5 days and 12h before analysis, additional media including stimulation was added after day 3 in IncuCyte.* ***B)*** *proliferation assays of MDA-MB-231, cells were incubated in IncuCyte for 3 days before analysis.* ***C)*** *WB of MCF7 cell lysates from proliferation assays.* ***D)*** *WB of MDA-MB-231cell cell lysates from proliferation assays.*

4.4.3 Dexamethasone treatment

It was of interest to compare GCs activation on the cell lines and observe the effects it would have on their proliferation and observe the molecular differences in the cells. Each cell line was stimulated with Ani (0,1 µg/ml, 10 µg/ml) and Dex (50nM, 100nM) and placed in In IncuCyte for monitoring. 3 pictures from each well were taken every 3 hrs. MCF7 cells were in IncuCyte for ca. 6 days and new media with stimulation was added after day 3 and mixed with old media. MDA-MB-231 cells were in IncuCyte for 3 days. After IncuCyte cells were then subjected to lysis buffer and prepared for WB. According to the proliferation assay, Dex treatment increased proliferation in both cell lines. The increase was more prominent in MDA-MB-231 than in MCF7 (Figure 12A and B). Dex concentration of 50 nM resulted in a slightly higher proliferation compared to 100 nM Dex. In both cell lines, GR expression was not observed (Figure 12 C and D), This means that the GR upon ligand binding has behaved as expected. A Downregulation of GR expression after Dex stimulation indicates that Dex is bound to GR, and GR is activated in the cells. (44) p-GR S226 appears to be slightly higher expressed in treated vs non-treated cells, indicating that Dex activates p-GR-226. This seems not to be the case for the MDA-MB-231 cells (Figure 12 D), since p-GR S226 is prominent in non-treated cells compared to treated cells

Activated p38 (p-p38) is observed for both cell lines (Figure 12C and D) at the end of the proliferation assays, there are some differences. MCF7 has uniform staining of p-p38 in non-treated and treated cells, indicating that the activation of the p38 pathway in this cell line is not affected by Dex, but is rather a product of the incubation conditions during the 5.5 day long proliferation assay (Figure 12C). However, for MDA-MB-231 cells there is an increase in p-p38 in the treated cells vs non-treated, indicating that Dex stimulation in these cells activates the p38 pathway (even after 3 days in culture). But since Dex is shown to increase cell proliferation, and since the Actin staining seems to be slightly increased in the Dex stimulated samples, it could also be that the Dex stimulated samples for MDA-MB-231 cells only contain more protein (Figure 12D). The difference in Actin of non-treated vs treated MCF7 cells do not show this same expression, reflecting the result of the proliferation assay, where Dex did not cause a major change in proliferation in these cells (Figure 12A). Confirming previous results (Figure 11C and D) HSP27 seems to be phosphorylated in the non-treated MCF7 cells, but not in the non-treated MDA MB 231 cells (Figure 12C and D). Stimuli with Dex did not change the pHSP27 status in either cell line. These results show that Dex increases proliferation to a larger degree in MDA-MB-231 cells compared to MCF7 cells. After several days in culture,

differences are also observed concerning the kinetics of p-GR S226 and p-p38 in response to Dex stimulation in the two cell lines.
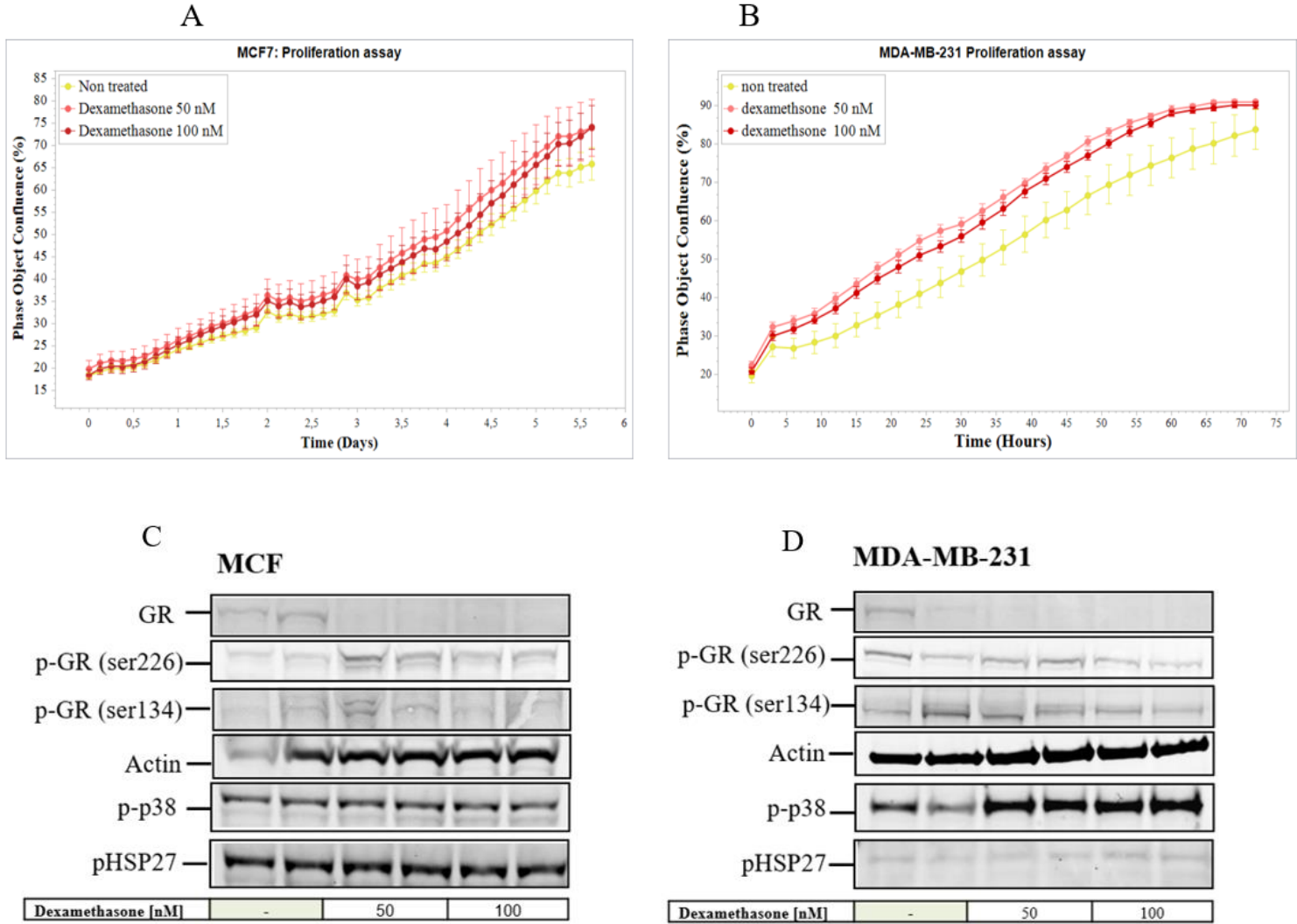

Figure 12: Dexamethasone treatment increased the proliferation in both cell lines. *Cells were stimulated with 50nM and 100nM Dex, then placed in IncuCyte and monitored according to their confluency. Cells from the proliferation assay were lysate and analyzed by WB. Non-treated cells were used as control. A) proliferation assays of MCF7, cells were incubated in IncuCyte for 5 days and 12hrs before analysis, additional media including stimulation was added after day 3 in IncuCyte. B) proliferation assays of MDA-MB-231, cells were incubated in IncuCyte for 3 days before analysis. C) WB of MCF7 cell lysates from proliferation assays. D) WB of MDA-MB-231cell lysates from proliferation assays.*

4.4.4 Anisomycin decreases cell viability

IncuCyte monitors cell proliferation based on cell confluence. According to the American Type Culture Collection (ATCC) MCF7 and MDA-MB-231 are classified as epithelial cells, but observations of the cells show that they have different morphology and growth pattern (APPENDIX I). MDA-MB-231 has more mesenchymal features(8) in its morphology and its growth pattern seems scattered. MCF7 are epithelial cells with a high degree of cell adhesion and the cells grow in colony. And because of the change in morphology and growth pattern. It was decided that cell proliferation should also be looked at with another method. CellTiter Glo is a method that monitors cell viability by measuring the metabolic activity in cells in culture. Each cell line was stimulated with Ani (0,1 µg /ml, 10 µg/ml) and Dex (50nM, 100nM). Starved cells were in media without FBS and insulin. Non-stimulated cells were used as control. In the first experiment, cells were stimulated for 30 min before they were harvested, and their ATP concentration was detected by use of the Cell Titer Glo kit and a Luminometer. 30 min detection did not have a detectable biological effect on the cells (Figure 13). In the second experiment, cells were therefore stimulated for 24 hrs and now differences in metabolic activity could be observed between non-stimulated and Ani and Dex stimulated cells for both cell types (Figure 13).

The non-treated cells are our controls. Ani stimulation decreased cell viability in both cell lines, compared to their non-treated cells. For both cell lines a 24 hrs stimulation of 10 µg/ml Ani gave the greatest inhibition with almost a 50% reduction in cell viability (Figure 13) compared to non-treated cells. For Dex treated cells the results were not similar in both cell lines. MDA-MB-231 cells seem to increase in the number of viable cells after Dex treatment, whilst there seems to be a slight reduction in MCF7 cells (Figure 13). However, most of the results in this assay seem to be in line with the results obtained for Ani and Dex treatment obtained by the IncuCyte experiments (Figure 11 and Figure 12), respectively. Starved cells were only added to this experiment because starvation affects proliferation too, and it was interesting to observe that MCF7 and MDA-MB-231 response to 0,1µg/ml Ani seemed to correspond to the same response exhibited by starved cells (Figure 13).
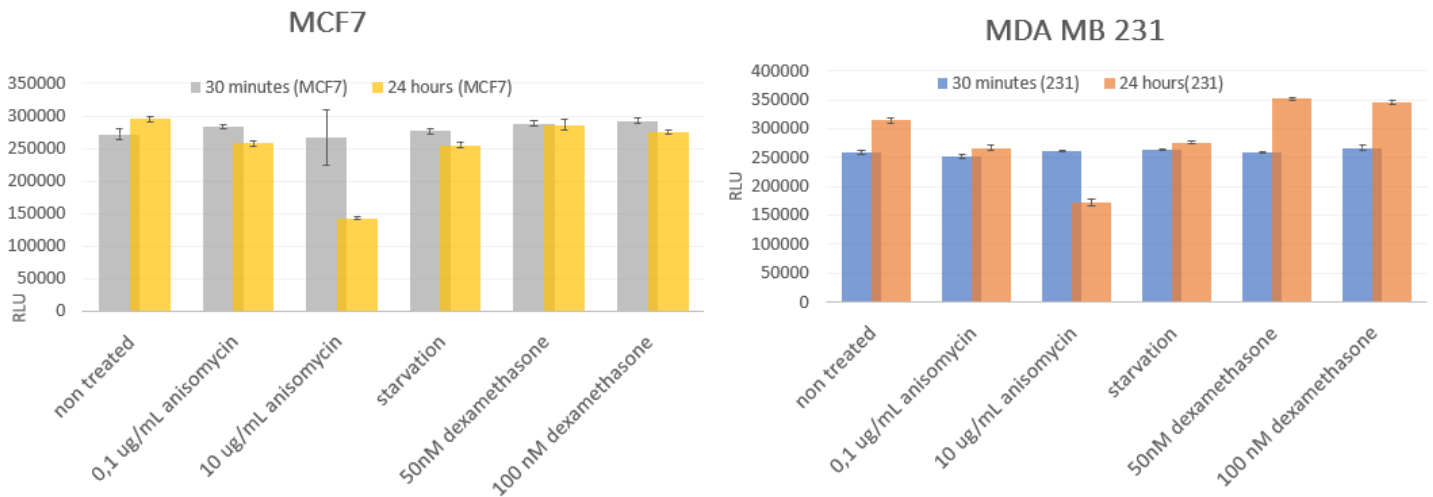
Figure 13: 24 hours stimulation of anisomycin and dexamethasone affects cell viability. Each cell line was starved or stimulated with 0,1µg/ml Ani, 10 µg/ml Ani, 50nM and 100nM Dex. Incubated for 30 min or 24 hrs. The cell viability assay was performed by CellTiter Glo and cells were detected by a Luminometer.

4.4.5 MCF7 and MDA-MB-231 exhibited differences in migration upon dexamethasone and Anisomycin stimulation

A cell migration assay can assist in revealing the capacity of cell motility and invasiveness toward a chemo-attractant gradient, respectively (1). Unlike basal cell line subtypes Luminal cell lines subtypes have less propensity to migrate due to tight cell-cell junctions (8), and MCF7 cells do not normally migrate or invade. (15) Therefore, it was of interest to detect the migration of MCF7 and MDA-MB-231 cells in response to Ani and Dex. To achieve this a scratch wound assay was conducted. A scratch by a WoundMaker was performed in a confluent cell layer, then cells were treated with Ani (0,1µg /ml, 10 µg/ml) and Dex (50nM, 100nM). Cell migration was monitored and analyzed by use of IncuCyte with 1 picture from each well taken every hr. MDA-MB-231 cells were left for 24 h, while MCF-7 cells were left for 5 days.

That 50 nM and 100 nM concentration of Dex decreased the migration of MDA-MB-231 cells, whilst it slightly increased migration in MCF7 cells. Ani stimulation decreased the migration

of MDA-MB-231 and MCF7 cells, with 10 µg/ml giving the greatest reduction in migration of MDA-MB-231 cells. The migration in MCF7 seems to mimic the effect of Dex and Ani on the proliferation assay (Figure 11A and Figure 12A), although the Dex effect only slightly increased MCF7 cells proliferation (Figure 12). This could also indicate that there is no migration in the MCF7 cells and that cells are just naturally proliferating. Both Dex and Ani seem to inhibit MDA-MB-231 cells migration.
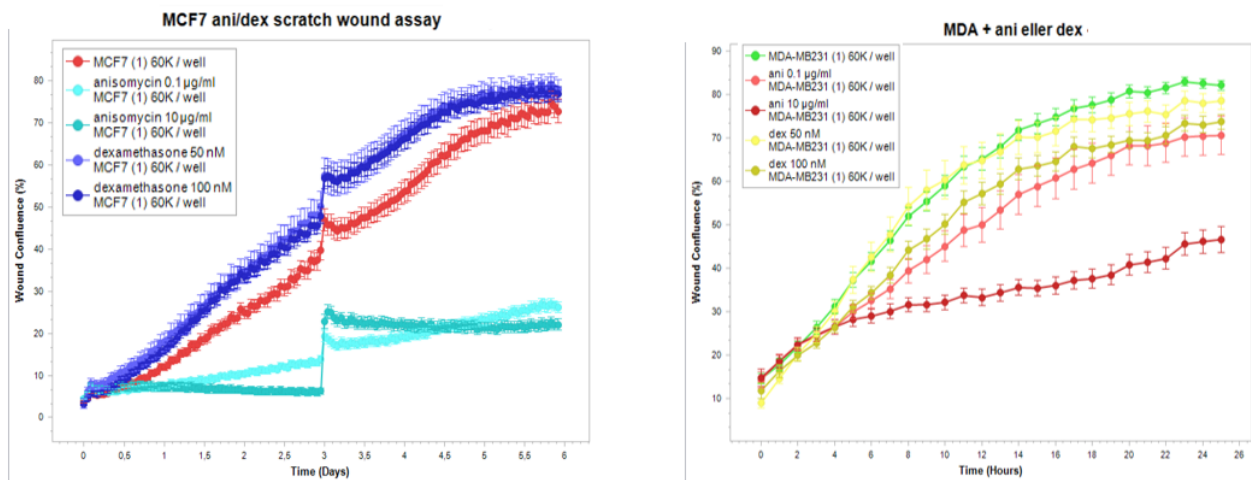

Figure 14: MDA-MB-231 migration is influenced by stimulations, MCF7 migration does not seem to be affected by the stimulations. Cells were seeded in a 96 well plate and stimulated with Dex (50nM, 100nM) and Ani (0,1 µg/mL- and 10 µg/mL). The scratch wound was made by a wound maker before stimulation and analyzed in Incucyte. MCF7 cells were in IncuCyte for 6 days, and more media with stimulation was added after the 3 days. MDA-MB-231 cells were in IncuCyte for 24 h.

4.5 MCF and MDA-MB-231 cell recovery study.

Results from this study confirm that Ani would inhibit proliferation, viability and migration for both cell types. As detected by the IncuCyte proliferation study (Figure 11A and B) stimulated cells appear to be on hold, showing no increase in growth (MDA-MB-231), or even a slight decrease (MCF7) in growth after Ani stimulation. The WB done at the end of the experiment indicated that cells incubated with the highest concentration of Ani (10 ug/ml) would ultimately die, as shown by the complete lack of proteins in the lysates (Figure 11C and D). However, what is happening with the cells exposed to 0.1 ug/ml Ani? Are they on hold? Have they

irreversibly left the cell cycle, or will they manage to recover and start proliferation as soon as Ani is removed? To find out, a cell recovery study was designed where each cell line was stimulated with low dose Ani (0,1 µg/ml) and Dex (50 nM) and had a recovery batch and a control batch. Control cells were stimulated for 24 hrs and then subjected to lysis buffer and prepared for WB. The recovery batch was stimulated for 24 h in IncuCyte and old media was taken away and new media without stimulation was added to cells and cells were in IncuCyte for an additional 3 days before cells were subjected to lysis buffer and prepared for WB.
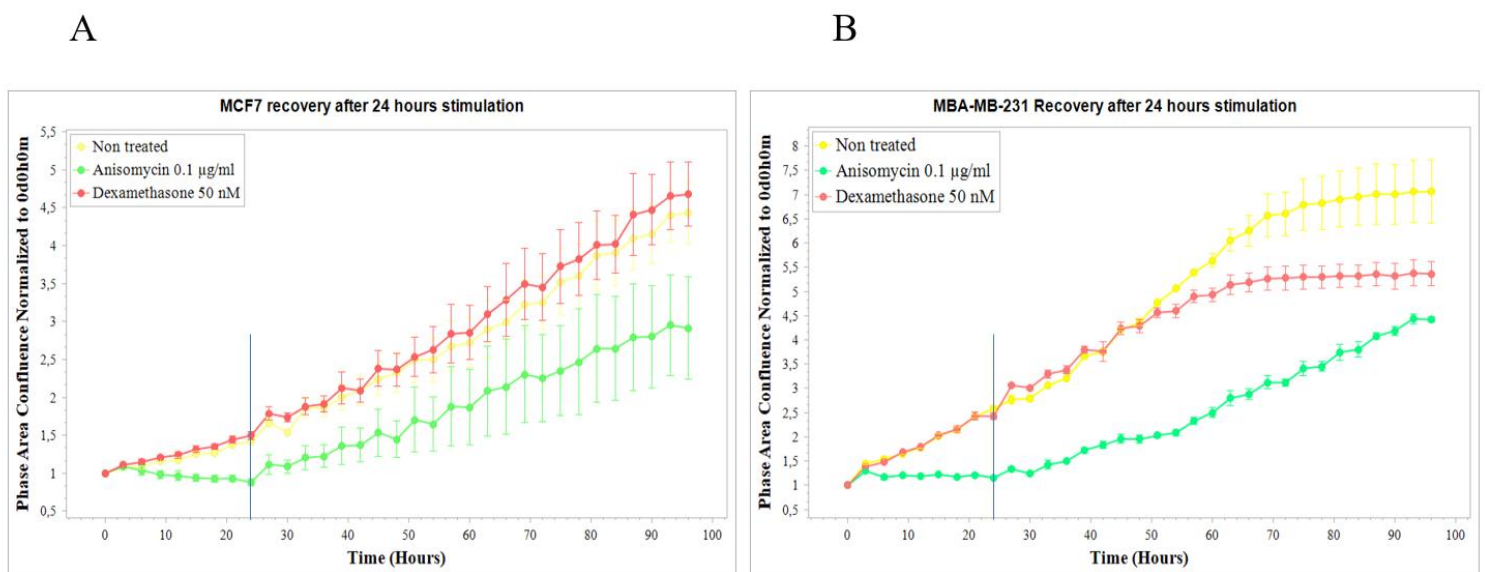
A

B

Figure 15: Cells proliferate as normal after recovery from anisomycin stimulation. MCF7 (left) and MDA-MB-231 (right). **1. Control cells**: *Each cell line was stimulated with Anisomycin: 0,1 µg/ml and Dexamethasone: 50nM for 24 hrs in incubator, before cell lysis. Non-treated cells were used as control.* **2.Recovery cells:** *Each cell line was stimulated with Anisomycin: 0,1 µg/ml and 50nM Dex for24 hrs in IncuCyte, then stimulations was taken away and new fresh media was added to the cells and monitored for an additional 3 days in IncuCyte before cell lysis. The line in the graf marks the end of the 24 h stimulation with Ani and Dex. Cells were lysated after 24 hrs (control cells), and cells were lysate after additional 3 days in incuCyte (recovery cells) were analysed by WB (Figure 16)*

The proliferation curves confirm the immediate and inhibitory effect of Ani treatment for both cell lines, indicated by a flat proliferation curve between 0 and 24 hrs (Figure 15). At this time point, the drug was removed, the cells were briefly washed before fresh media without the drug was added, and the incubation continued. Interestingly, for both cell lines, the removal of Ani was sufficient to initiate proliferation again, indicating that the drug had caused no irreversible

changes (Figure 15). These results showed that cells proliferate as normal after recovery from Ani treatment

DNA damage detection before and after cell recovery

It was of interest to detect if the Ani stimulation could induce DNA damage and/or changes in the cell cycle. Furthermore, Dex is known to induce DNA damage (49, 50) so it would be interesting to have a look at the effect of Dex treatment in this regard as well. Western blot was done on cell lysates prepared 24 hrs after stimulation with drugs and after 3 days of recovery as described in Figure 15. In addition, extracts stimulated for 30 min were included to visualize the effect of short-term stimulation. Proliferation is interconnected with the cell cycle (51) The main function of the tumor-suppressor protein p53 is induction of apoptosis and cell cycle arrest. It is also involved in DNA repair. Since the ER-positive MCF7 has wild-type p53 and the TNBC MDA-MB-231 cells have a mutant p53 protein, differences in the responses to DNA damage could be expected. Antibodies used for the WB were yH2Ax, cyclin D1 and D3. Histone H2Ax is phosphorylated to yH2Ax, upon DNA double-stranded breaks and is used for DNA damage detection (52). The cyclins are important proteins that aid cell cycle progression from the G1 phase to the S phase. (51)

The two lanes to the right on each blot show how the yH2Ax, cyclin D1 and D3 stainings would look when DNA damage is induced by UV light for each cell line (Figure 16). There is a clear induction of yH2Ax and reduction of cyclinD1for both cell lines, while the expression of cyclin D3 differs, it is not affected by DNA damage in the MCF7 cells while it is reduced in the MDA-MB-231 cells. For short-term stimulation with Ani (30 min), it seems that both yH2Ax, cyclin D1 and D3 are induced to a larger degree in the MDA-MB-231 cells compared to the MCF 7 cells (the lanes to the left on each blot in Figure 16A and B). Dex stimulation for 30 min did not have any effect on either of the cell lines. However, at 24 hrs incubation with the drugs, it is the opposite. Here, Ani stimulation has no effect on the expression of yH2Ax, cyclin D1 and D3, while Dex treatment causes a slightly increased expression of these proteins for both cell lines (Figure 16). The most surprising result is observed for the samples from the recovery cells (the cells were incubated with the drugs for 24 hrs before the drugs were removed and the cells were incubated for 3 more days for recovery). Here the expression of cyclinD1 and D3 is increased for both cell types and the increase seems to be a bit more for the Dex treated cells compared to the Ani treated. Cells have been left proliferating for 3 days so the Actin staining is also a bit elevated, but it cannot account for the observed difference in expression of yH2Ax,

cyclin D1 and D3 between Dex and Ani treated samples. Ani thus seems to induce elevated expression of these three proteins after 30 min, while for Dex the induction appears later and seems to last even when the drug is removed. Activation of p38 is similar in the two cell lines after UV induction but differs in response to the drug treatment. MCF7 has very low background levels of p-p38, and p-p38 is heavily induced after 30 min Ani stimulation. No p-p38 staining is visible on the WB after 24 hrs or 3 days of recovery (Figure 16). For MDA-MB-231 cells a weak background level of p-p38 can be observed in unstimulated cells and the p-p38 is not as powerfully induced by ani stim for 30 min as it was for MCF7. However, for MDA-MB-231 cells p-p38 is still visible in the 3 day recovery extract. Unfortunately, it is not possible to compare the p-p38 staining between the Ani and Dex treated cells here.
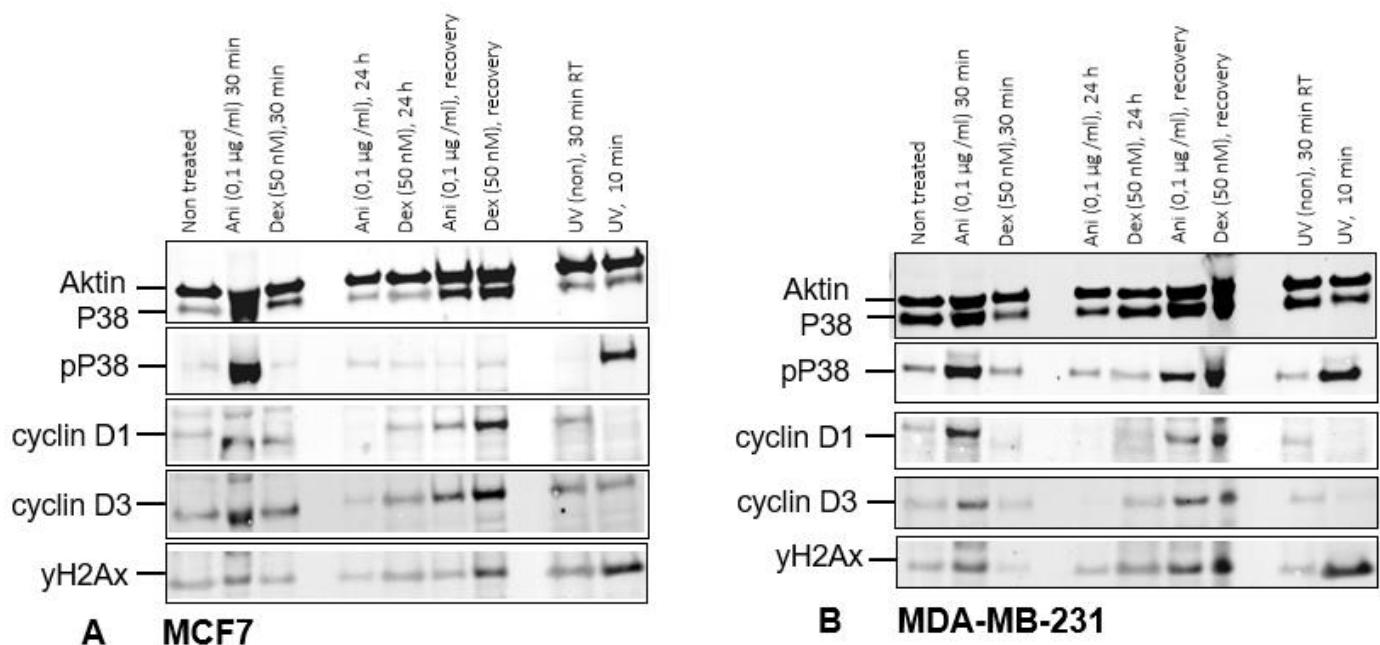

*Figure 16: MDA-MB-231 and MCF7 recovery cells have different signals of p38 and p- p38. Western Blot for DNA damage detection. These blots consist of multiple cell lysates. **Ani and Dex stimulated Control cells:** Each cell line was stimulated with Anisomycin: 0,1 µg/ml and Dexamethasone: 50nM for 30 min in an incubator, before cell lysis. **Control cells from recovery study:** Each cell line was stimulated with Anisomycin: 0,1 µg/ml and Dexamethasone: 50nM for 24 hrs in an incubator, before cell lysis. **Recovery cells:** Each cell line was stimulated with Anisomycin: 0,1 µg/ml and Dexamethasone: 50nM for 24 hrs in IncuCyte, then stimulations were taken away and new fresh media was added to the cells and monitored for an additional 3 days in IncuCyte before cell lysis. **UV cells:** Each cell line was stimulated to UV for 10 minutes and cells at room temperature (RT) were used as a control for UV stimulated cells. Non-treated cells were used as a control on the WB.*

5 Discussion

This thesis aims to observe and discover differences in responses of the two breast cancer cell lines MCF7 and MDA-MB-231 activation of the p38 MAPK pathway and GR. To study this, stimulation with Ani and Dex was used and effects were observed by implementing molecular and biological methods. The breast cancer cell lines consist of cell-specific attributes, MCF7 is ER+ and PR+, these belong to the luminal cell line subtype. MBA-MB 231 is ER-, PR- and HER2- and belongs to the basal B cell line subtype (8). Provided with differences in their molecular composition, it would be natural to expect different responses between the cell lines. Subsequently, this study found some molecular and biological similarities and differences in the cell lines' response to Ani and Dex stimulation. This discussion will comment on the cell proliferation and discuss the obtained results regarding Ani and Dex activation of the p38 and GR pathway. The similarities and differences in the cells regarding the p38 MAPK and GR. In conclusion, this discussion will end with some speculations and reflective thought on the potential applications and studies in the future.

The general proliferation status of MCF7 and MDA-MB-231 shows that MDA-MB-231 cells had an increased proliferation rate according to confluency compared to MCF7 cells (Figure 10). IncuCyte was used to extract this data, however the IncuCyte exhibits proliferation in terms of confluency. MCF7 grows in colonies, whilst MDA-MB-231 growth is more spread throughout a surface (Appendix). This difference in growth could affect the confluency of the cells, automatically giving MDA-MB-231 cells a higher confluency than MCF7cells and resulting into MDA-MB-231 having an increased growth compared to MCF7 cells. Hence, the IncuCyte could give an inaccurate proliferation status. This is because, the number of cells would not directly correspond to its confluency when the growth profiles are different. Proliferation was also measured by another method known as CellTiter Glo, which measures metabolic activity. Here, there were also observed differences between the two cell lines, with MDA-MB-231 cells being slightly more metabolically active than MCF7 after 24 hrs. (Figure 13, non-treated cells). This also indicates an increased proliferation rate. While the morphology and growth pattern makes it difficult to directly compare the proliferation rate of the two cell lines by use of IncuCyte, this method is still valid to detect changes in proliferation and migration within each cell line after drug stimuli and that is what is done in this project.

5.1 Activation of p38 MAPK

The p38 pathway is activated in response to stress and has multiple functions upon activation. The p38 MAPK can control cell growth and apoptosis (27). Functionally, the localization of p-p38 and GR was investigated (Figure 9). Unfortunately, p-p38 was difficult to detect, but it has been reported to be detected in the cytosol and nucleus (30). In the present study, Ani rapidly activates the p38 MAPK in both cell lines shown in Figure 6. The phosphorylation of GR S134 followed by the activation of the p38 MAPK signaling pathway indicated by Figure 6 has been reported by other experts to be dependent on p-p38 (40, 45, 46). Phosphorylated Ser134 is reported to inhibit GR function, resulting in an impaired GR nuclear translocation (41), but it is also reported to cause transcriptional activation of a subset GR target genes (40, 41). This project confirms that the activation of p38 MAPK promotes GR Ser134 phosphorylation. p-GR S134 function is to impair GR nuclear translocation and/or transcriptional activation of a subset of GR target genes (41) as well as the cross-talk between p38 MAPK. This is observed in both MDA-MB-231 and MCF7 cells. This is interesting since it is suggested that p-GR S134 obtained the ability to exhibit unique oncogenic functions in breast cancer cooperatively with p38 MAPK(40, 46). We observed that Ani stimulation causes activation of p38 MAPK and p-GR S134. Furthermore, the Ani stimulation resulted in decreased proliferation (Figure 11), decreased cell viability (Figure 13) and decreased migration (Figure 14) in both cell lines. The effect the Ani stimulation had on cell proliferation was reversible since MDA-MB-231 and MCF7 cells were able to recover after 24 hrs of Ani stimulation (Figure 15)

The activation of p38 MAPK triggers downstream substrates such as MK2 and HSP27(32, 53). In this study, MK2 was not looked at. However, its downstream target pHSP27 was used as a read-out for MK2 activity since phosphorylation of HSP27 is directly dependent on MK2 activity (32). A high expression of HSP27 contributes to the progression of malignant behaviour in multiple cancers(54). Therefore, it is considered a potential target for the treatment of breast cancer (31, 32, 55). The levels of pHSP27 were different in the two cell lines (Figure 11 and Figure 12). This is a clear indication that the p38 MAPK pathway is a different downstream of activated p38 in these cell lines. HSP27 is also known to inactivate p53(54). Therefore, it is worth noting that MDA-MB-231 has mutant p53 and MCF7 has wild type p53. The increased activation of HSP27 observed in MCF7 cells compared to MDA-MB-231 is therefore

anticipated to influence p53 activity in these cells. Ani treatment seemed to reduce HSP27 activation in MCF7 after prolonged incubation (Figure 11). This means that the cells are inactivating p53 and in a cell surviving mode. Ani cell surviving role through HSP27 appears to be opposite to the results in the proliferation assay (Figure 11). However, p38 MAPK is complex. P38 isoforms can promote both pro-oncogenic and tumor suppressive processes (27). Activity in p38 depend on cell type differences along with the duration, quality and intensity of the stimulus, its communication and interaction with other signaling pathways (27). In the recovery study, the WBs show a difference in the expression of p38 and p-p38 in MCF7 and MDA-MB-231 (Figure 16). p38 seems to be more expressed in MDA-MB-231, regardless of the stimuli compared to MCF7 cells. In addition, the signals of p-p38 are more visible in MDA-MB-231 and prominent in recovery cells compared to MCF7(Figure 16). The difference is also noticeable in the proliferation assay (Figure 11). This difference in kinetics of p38 MAPK is not the same for bothMCF7 and MDA-MB-231 cells.

5.2 GR in MCF and MDA-MB-231

GR has multiple functions as well, including effects on cell metabolism, differentiation, stress responses, proliferation, apoptosis, and survival (1, 43). GR lies in the cytosol of the cell and there was a clear difference in GR localization between MCF7 and MDA-MB-231 (Figure 9). In non-treated MCF7cells, the majority of GR was localized in the cytosol as expected. For MDA-MB-231, GR seems to be localized in the nucleus (Figure 9), the observations were unexpected. This is because GR translocation to nucleus is ligand-dependent (43). However, it is reported by others that altered GR localization and GR post translational modification in individual breast cancer cells contributes to heterogeneity (40). Although unliganded GR nuclear translocation is still not completely understood. Several studies have shown that GR can be activated in the absence of ligands(56).

Moreover, it is reported that GR expression in TNBC predicts poor prognosis and high GR expression in ER-positive breast cancer is associated with a good prognosis (40). In a previous study, survival rates of GR-high patients in TNBC and invasive subtypes were significantly reduced(57). GR activation upon synthetic GCs has been observed to increase tumors and metastasis (1, 40). Our results show that MDA-MB-231 cells have increased proliferation upon Dex activation (Figure 12). Our results are in line with previous results. Studies have shown

that GR interacts with ER in ER-positive breast cancer cells and seems to inhibit ER-dependent genes important for proliferation (58). GR activation is antiapoptotic in cancer cells lacking ER, whereas ER-positive cells have a GR/ER cross-talk that contributes to improved outcomes in high GR-expressing tumors (59). MCF7 cells have an ER-dependent proliferation and GR is shown to modify ERs transcriptional function so that it acts less tumorigenic (40) and this could be an explanation for the decrease in cell viability. In this study, experiments were done without the addition of estrogen but an even more clear function of Dex in modifying proliferation could have been observed if estrogen had been added.

Results from the Dex titration study shows that, the concentration of ≥100 nM MCF7 have non or fewer signals of GR and p-GR forms compared to MDA-MB-231 (Figure 8). No signals of GR upon GCs ligand-binding is linked to a complete GR activation and ubiquitylation leading to proteasomal degradation (44). In IF, it was possible to see GR in MCF7 cells in nucleus but it was still not as prominent as MDA-MB-231 (Figure 9). GR was still heavily expressed in MCF7 cells cytosol. This might suggest that, 100nM Dex would be more efficient in translocating GR to the nucleus in MCF7 cells. MDA-MB-231 expresses GR. However, the signal decreases with increasing Dex concentrations (Figure 8). It was also observed that the lowest concentration of Dex (1 nm) seemingly induced phosphorylation of S134, whilst higher doses of Dex did not have any effect (Figure 8). Dex did not cause any difference in p-S134 in MCF cells. However, lower doses of Dex was able to induce p-GR S226 on GR. The GR S226 residue is known to be activated by JNK and enhances its nuclear export after withdrawal of a ligand for GR, such as dexamethasone. So, a S226 reduction could indicate that a ligand binding is taking place (60).

Consequently, results from this study show the crosstalk between the p38 MAPK and GR upon Ani stimulation. It is also indicated through our results that the kinetics of the crosstalk might be different. In TNBC it is shown that p-GR S134 was linked to cell cycle survival and migration in TNBC cells. It is also suggested that p38 MAPK induced p-GR S134, is crucial for TNBC oncogenic actions.(46). According to a previous report p-GR S134 is increased in TNBC compared to luminal cases (40). Our results revealed that in accordance with the scratch wound assay MDA-MB-231 cells migration was influenced upon stimuli. It has been reported that Dex increases migration(1, 40), but our observations show the inverse.

5.3 Anisomycin recovery

In the recovery study, it shows that a short-term Ani treatment -30 min gave an increased signal of p-p38 whilst a prolonged Ani treatment-24 hrs gave no signals of p-p38 (Figure 16). This could indicate that Ani activation of the p38 MAPK is temporary, and we could speculate if Ani mechanism of action is not through the p38 MAPK, since other studies have found underlying mechanism of Ani(35, 36). Furthermore, p38 can also control cell cycle progression, through the G1/S and G2/M check points and can promote the down-regulation of cyclin D1 (47). In addition, results from the recovery study showed an increase in cyclin D1 and D3 with short-term Ani treatment in both cell lines but a decrease or no signal upon prolonged Ani treatment. The down regulation of the cyclin would mean cell cycle arrest event though it is interesting to observe that this is not caused by an activation of the p38 MAPK. In both cell lines UV stimulated cells is a down regulation of the cyclins upon an p- p38. This again could indicate that Ani might have another mechanism.

In the recovery study, yH2Ax is known as a DNA double strand break marker, and is used to detect DNA damage (52). In the cells, DNA damage would be handled differently because of the differences in p53. We can observe a slight difference in DNA damage detection between the Ani stimulated recovery cells (Figure 16). MCF seem to recover compared to MDA-MB-231 and MDA-MD-231 p38 MAPK is still activated in the recovery cells, indicating that recovery is still not completed. This is not the same in both cell lines.

6 Conclusion

Anisomycin and Dexamethasone stimulations were used to study activation of the p38 MAPK signaling pathway and activation of GR in MCF7 (ER and PR-positive) and MBA-MB 231 (ER-, PR- and HER2-negative) breast cancer cell lines. The results show that they do respond differently. A low concentration of Ani (0,1 µg/ ml) rapidly activated the p38 MAPK and inhibited proliferation in both cell lines. This inhibition was reversible if the drug was removed after 24 hrs. Activated p38 MAPK and the cross-talk with p-GR (ser134) was visible in both cell lines but the kinetics was different. It was also observed that the level of phosphorylated HSP27 was different, indicating that downstream components in the p38 MAPK signaling pathway may differ between the cell lines.

Dex activated GR in both cell lines, but the response to GR activation was different. Dex increased proliferation in MDA-MB-231 cells, whilst MCF7 was not as affected by activation of GR compared to MDA-MB-231 cells. This thesis shows that there are molecular and functional differences between this cell lines in response to activation of the p38 MAPK and GR. A further understanding of the differences could be exploited and used in advancing targeted therapy.

7 References

1.   Pang JM, Huang Y-C, Sun S-P, Pan Y-R, Shen C-Y, Kao M-C, et al. Effects of synthetic glucocorticoids on breast cancer progression. Steroids. 2020;164:108738.
2.   Organisation WH. Breast Cancer World Health Organisation; 2021 [Fact sheet]. Available from: https://www.who.int/news-room/fact-sheets/detail/breast-cancer#:~:text=Scope%20of%20the%20problem%20In%202020%2C%20there%20were,years%2C%20making%20it%20the%20world%E2%80%99s%20most%20prevalent%20cancer.
3.   DeSantis CE, Bray F, Ferlay J, Lortet-Tieulent J, Anderson BO, Jemal A. International Variation in Female Breast Cancer Incidence and Mortality Rates. Cancer Epidemiol Biomarkers Prev. 2015;24(10):1495-506.
4.   Orchard GN, Brain Cell structure and function. Great Clarendon Street, Oxford, OX2 6DP, United Kingdom: Oxford university press; 2015. 500 p.
5.   Mammary Glands: National Cancer Institute; [Available from: https://training.seer.cancer.gov/anatomy/reproductive/female/glands.html.
6.   Camarillo IG, Xiao F, Madhivanan S, Salameh T, Nichols M, Reece LM, et al. 4 - Low and high voltage electrochemotherapy for breast cancer: an in vitro model study. In: Sundararajan R, editor. Electroporation-Based Therapies for Cancer: Woodhead Publishing; 2014. p. 55-102.
7.   Klevos GA, Ezuddin NS, Vinyard A, Ghaddar T, Gort T, Almuna A, et al. A Breast Cancer Review: Through the Eyes of the Doctor, Nurse, and Patient. Journal of Radiology Nursing. 2017;36(3):158-65.
8.   Dai X, Cheng H, Bai Z, Li J. Breast Cancer Cell Line Classification and Its Relevance with Breast Tumor Subtyping. J Cancer. 2017;8(16):3131-41.
9.   Skor MN, Wonder EL, Kocherginsky M, Goyal A, Hall BA, Cai Y, et al. Glucocorticoid Receptor Antagonism as a Novel Therapy for Triple-Negative Breast Cancer. Clinical Cancer Research. 2013;19(22):6163.
10.   Welsh J. Chapter 40 - Animal Models for Studying Prevention and Treatment of Breast Cancer. In: Conn PM, editor. Animal Models for the Study of Human Disease. Boston: Academic Press; 2013. p. 997-1018.
11.   Ahmad A. Breast Cancer Metastasis and Drug Resistance: Challenges and Progress. Cham: Cham: Springer International Publishing AG; 2019.
12.   Jerez Y, Márquez-Rodas I, Aparicio I, Alva M, Martín M, López-Tarruella S. Poly (ADP-ribose) Polymerase Inhibition in Patients with Breast Cancer and BRCA 1 and 2 Mutations. Drugs. 2020;80(2):131-46.
13.   Bianchini G, De Angelis C, Licata L, Gianni L. Treatment landscape of triple-negative breast cancer - expanded options, evolving needs. Nat Rev Clin Oncol. 2021.
14.   Keung MY, Wu Y, Badar F, Vadgama JV. Response of Breast Cancer Cells to PARP Inhibitors Is Independent of BRCA Status. Journal of Clinical Medicine. 2020;9(4).
15.   ComŞA Ş, CÎMpean AM, Raica M. The Story of MCF-7 Breast Cancer Cell Line: 40 years of Experience in Research. Anticancer Research. 2015;35(6):3147.
16.   Cooper GM, Hausman RE. The cell : a molecular approach. 7th ed. Sunderland, Massachusetts: Oxford University Press; 2018.
17.   Alberts B, Hopkin K, Johnson A, Morgan D, Raff M, Roberts K, et al. Essential cell biology. Fifth edition.; International student edition. ed. New York,London: W. W. Norton & Company; 2019.
18.   Thu KL, Soria-Bretones I, Mak TW, Cescon DW. Targeting the cell cycle in breast cancer: towards the next phase. Cell Cycle. 2018;17(15):1871-85.

19.   Stewart ZA, Pietenpol JA. p53 Signaling and Cell Cycle Checkpoints. Chemical Research in Toxicology. 2001;14(3):243-63.
20.   Levine AJ. p53: 800 million years of evolution and 40 years of discovery. Nat Rev Cancer. 2020;20(8):471-80.
21.   Kastenhuber ER, Lowe SW. Putting p53 in Context. Cell. 2017;170(6):1062-78.
22.   Levine AJ. P53 and The Immune Response: 40 Years of Exploration-A Plan for the Future. Int J Mol Sci. 2020;21(2).
23.   Hu J, Cao J, Topatana W, Juengpanich S, Li S, Zhang B, et al. Targeting mutant p53 for cancer therapy: direct and indirect strategies. Journal of Hematology & Oncology. 2021;14(1):157.
24.   Stramucci L, Pranteda A, Bossi G. Insights of Crosstalk between p53 Protein and the MKK3/MKK6/p38 MAPK Signaling Pathway in Cancer. Cancers. 2018;10(5):131.
25.   Gutierrez-Prat N, Cubillos-Rojas M, Cánovas B, Kuzmanic A, Gupta J, Igea A, et al. MK2 degradation as a sensor of signal intensity that controls stress-induced cell fate. Proceedings of the National Academy of Sciences. 2021;118(29):e2024562118.
26.   Lee MJ, Yaffe MB. Protein Regulation in Signal Transduction. Cold Spring Harb Perspect Biol. 2016;8(6).
27.   García-Hernández L, García-Ortega MB, Ruiz-Alcalá G, Carrillo E, Marchal JA, García MÁ. The p38 MAPK Components and Modulators as Biomarkers and Molecular Targets in Cancer. International Journal of Molecular Sciences. 2022;23(1):370.
28.   Xu W, Liu R, Dai Y, Hong S, Dong H, Wang H. The Role of p38γ in Cancer: From review to outlook. International Journal of Biological Sciences. 2021;17(14):4036-46.
29.   Lee S, Rauch J, Kolch W. Targeting MAPK Signaling in Cancer: Mechanisms of Drug Resistance and Sensitivity. International Journal of Molecular Sciences. 2020;21(3):1102.
30.   Wood CD, Thornton TM, Sabio G, Davis RA, Rincon M. Nuclear Localization of p38 MAPK in Response to DNA Damage. International Journal of Biological Sciences. 2009;5(5):428-37.
31.   Choi S-K, Kam H, Kim K-Y, Park SI, Lee Y-S. Targeting Heat Shock Protein 27 in Cancer: A Druggable Target for Cancer Treatment? Cancers. 2019;11(8).
32.   Wang J, Wang G, Cheng D, Huang S, Chang A, Tan X, et al. Her2 promotes early dissemination of breast cancer by suppressing the p38-MK2-Hsp27 pathway that is targetable by Wip1 inhibition. Oncogene. 2020;39(40):6313-26.
33.   Grollman AP. Inhibitors of Protein Biosynthesis: II. MODE OF ACTION OF ANISOMYCIN. Journal of Biological Chemistry. 1967;242(13):3226-33.
34.   Wang Q, Kong L, Zheng X, Shen J, Wang J, Zhang D, et al. Acyltransferase AniI, a Tailoring Enzyme with Broad Substrate Tolerance for High-Level Production of Anisomycin. Applied and Environmental Microbiology. 2021;87(14):e00172-21.
35.   Tan H, Hu B, Xie F, Zhu C, Cheng Z. Anisomycin sensitizes non-small-cell lung cancer cells to chemotherapeutic agents and epidermal growth factor receptor inhibitor via suppressing PI3K/Akt/mTOR. Fundamental & Clinical Pharmacology. 2021;35(5):822-31.
36.   Zhang C, Deng Q, Bao S, Zhu J. Anisomycin is active in preclinical models of pediatric acute myeloid leukemia via specifically inhibiting mitochondrial respiration. J Bioenerg Biomembr. 2021;53(6):693-701.
37.   Lee K-H, Nishimura S, Matsunaga S, Fusetani N, Ichijo H, Horinouchi S, et al. Induction of a Ribotoxic Stress Response That Stimulates Stress-Activated Protein Kinases by 13-Deoxytedanolide, an Antitumor Marine Macrolide. Bioscience, Biotechnology, and Biochemistry. 2006;70(1):161-71.
38.   Charmandari E, Kino T, Chrousos GP. Glucocorticoid Receptor. In: Martini L, editor. Encyclopedia of Endocrine Diseases. New York: Elsevier; 2004. p. 229-34.
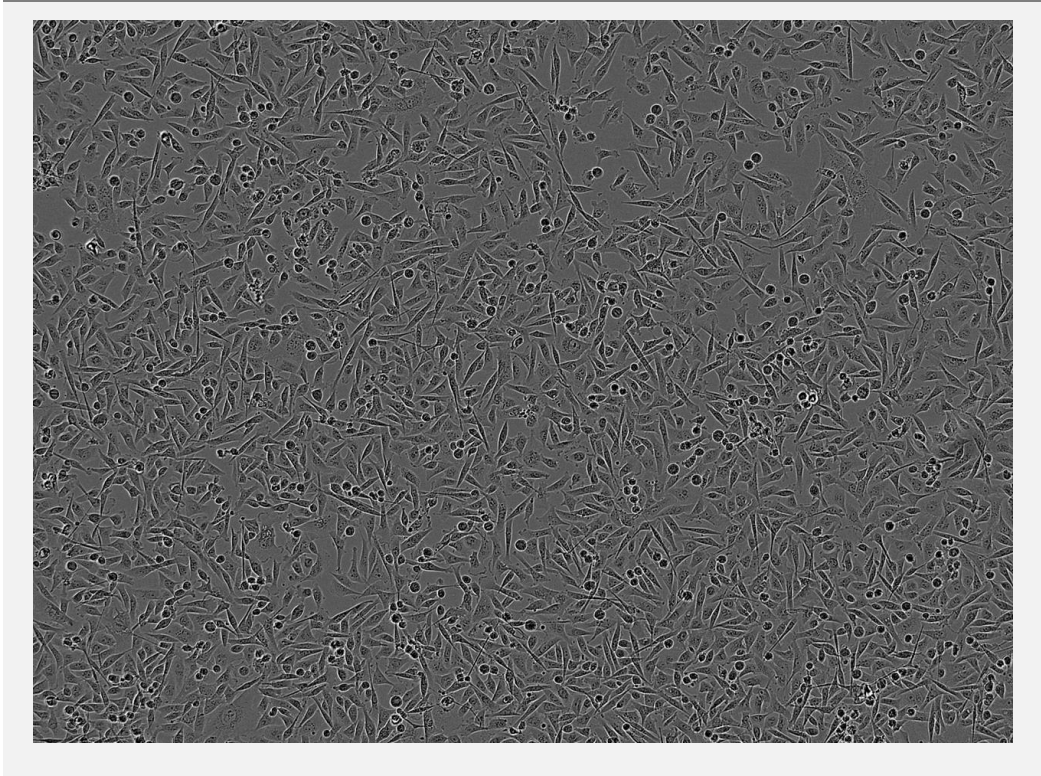
39.	Timmermans S, Souffriau J, Libert C. A General Introduction to Glucocorticoid Biology. Frontiers in Immunology. 2019;10.

40.	Kerkvliet Carlos P, Truong Thu H, Ostrander Julie H, Lange Carol A. Stress sensing within the breast tumor microenvironment: how glucocorticoid receptors live in the moment. Essays in Biochemistry. 2021;65(6):971-83.

41.	Sevilla LM, Jiménez-Panizo A, Alegre-Martí A, Estébanez-Perpiñá E, Caelles C, Pérez P. Glucocorticoid Resistance: Interference between the Glucocorticoid Receptor and the MAPK Signalling Pathways. International Journal of Molecular Sciences. 2021;22(18).

42.	Oakley RH, Cidlowski JA. The biology of the glucocorticoid receptor: New signaling mechanisms in health and disease. Journal of Allergy and Clinical Immunology. 2013;132(5):1033-44.

43.	Lesovaya EA, Chudakova D, Baida G, Zhidkova EM, Kirsanov KI, Yakubovskaya MG, et al. The long winding road to the safer glucocorticoid receptor (GR) targeting therapies. Oncotarget. 2022;13(1).

44.	Wallace AD, Cidlowski JA. Proteasome-mediated Glucocorticoid Receptor Degradation Restricts Transcriptional Signaling by Glucocorticoids*. Journal of Biological Chemistry. 2001;276(46):42714-21.

45.	Zeyen L, Seternes OM, Mikkola I. Crosstalk between p38 MAPK and GR Signaling. International Journal of Molecular Sciences. 2022;23(6):3322.

46.	Perez Kerkvliet C, Dwyer AR, Diep CH, Oakley RH, Liddle C, Cidlowski JA, et al. Glucocorticoid receptors are required effectors of TGFβ1-induced p38 MAPK signaling to advanced cancer phenotypes in triple-negative breast cancer. Breast Cancer Research. 2020;22(1):1-23.

47.	Martínez-Limón A, Joaquin M, Caballero M, Posas F, de Nadal E. The p38 Pathway: From Biology to Cancer Therapy. International Journal of Molecular Sciences. 2020;21(6):1913.

48.	Morgan D, Berggren KL, Spiess CD, Smith HM, Tejwani A, Weir SJ, et al. Mitogen-activated protein kinase-activated protein kinase-2 (MK2) and its role in cell survival, inflammatory signaling, and migration in promoting cancer. Mol Carcinog. 2022;61(2):173-99.

49.	Sengupta S, Wasylyk B. Ligand-dependent interaction of the glucocorticoid receptor with p53 enhances their degradation by Hdm2. Genes Dev. 2001;15(18):2367-80.

50.	Reeder A, Attar M, Nazario L, Bathula C, Zhang A, Hochbaum D, et al. Stress hormones reduce the efficacy of paclitaxel in triple negative breast cancer through induction of DNA damage. British Journal of Cancer. 2015;112(9):1461-70.

51.	Kashyap D, Garg VK, Sandberg EN, Goel N, Bishayee A. Oncogenic and Tumor Suppressive Components of the Cell Cycle in Breast Cancer Progression and Prognosis. Pharmaceutics. 2021;13(4).

52.	KUO LJ, YANG L-X. γ-H2AX - A Novel Biomarker for DNA Double-strand Breaks. In Vivo. 2008;22(3):305-9.

53.	Yao Y, Cui L, Ye J, Yang G, Lu G, Fang X, et al. Dioscin facilitates ROS-induced apoptosis via the p38-MAPK/HSP27-mediated pathways in lung squamous cell carcinoma. International Journal of Biological Sciences. 2020;16(15):2883-94.

54.	Lampros M, Vlachos N, Voulgaris S, Alexiou GA. The Role of Hsp27 in Chemotherapy Resistance. Biomedicines. 2022;10(4).

55.	O'Callaghan-Sunol C, Gabai VL, Sherman MY. Hsp27 Modulates p53 Signaling and Suppresses Cellular Senescence. Cancer Research. 2007;67(24):11779-88.

56.	Scheschowitsch K, Leite J, Assreuy J. New insights in glucocorticoid receptor signaling – more than just a ligand binding receptor. Frontiers in Endocrinology. 2017;8.

57.   Shi W, Wang D, Yuan X, Liu Y, Guo X, Li J, et al. Glucocorticoid receptor–IRS-1 axis controls EMT and the metastasis of breast cancers. Journal of Molecular Cell Biology. 2019;11(12):1042-55.

58.   Tonsing-Carter E, Hernandez KM, Kim CR, Harkless RV, Oh A, Bowie KR, et al. Glucocorticoid receptor modulation decreases ER-positive breast cancer cell proliferation and suppresses wild-type and mutant ER chromatin association. Breast Cancer Research. 2019;21(1):82.

59.   West DC, Kocherginsky M, Tonsing-Carter EY, Dolcen DN, Hosfield DJ, Lastra RR, et al. Discovery of a Glucocorticoid Receptor (GR) Activity Signature Using Selective GR Antagonism in ER-Negative Breast Cancer. Clin Cancer Res. 2018;24(14):3433-46.

60.   Itoh M, Adachi M, Yasui H, Takekawa M, Tanaka H, Imai K. Nuclear Export of Glucocorticoid Receptor is Enhanced by c-Jun N-Terminal Kinase-Mediated Phosphorylation. Molecular Endocrinology. 2002;16(10):2382-92.

APPENDIX I

IncuCyte pictures of the morphology of non-stimulated MCF7 and MDA-MB-231 after 3 days in IncuCyte

MDA-MB-231 cells

MC7 CELLS